

U–Pb baddeleyite ages, distribution and geochemistry of 925 Ma mafic dykes and 900 Ma sills in the North China craton: Evidence for a Neoproterozoic mantle plume

Peng Peng ^{a,*}, Wouter Bleeker ^b, Richard E. Ernst ^c, Ulf Söderlund ^d, Vicki McNicoll ^b

^a State Key Laboratory of Lithospheric Evolution, Institute of Geology and Geophysics, Chinese Academy of Sciences, Beijing 100029, China

^b Geological Survey of Canada, Ottawa, Canada K1A 0E9

^c Department of Earth Sciences, Carleton University, and Ernst Geosciences, 43 Margrave Avenue, Ottawa, Ontario, Canada K1T 3Y2

^d Department of Earth and Ecosystem Sciences, Lund University, Sölvegatan 12, SE-223 62 Lund, Sweden

ARTICLE INFO

Article history:

Received 14 July 2011

Accepted 30 August 2011

Available online 10 September 2011

Keywords:

Baddeleyite U–Pb age

North China craton

Mafic dyke swarm

Subcontinental lithospheric mantle

Neoproterozoic

Mantle plume

ABSTRACT

Numerous Neoproterozoic mafic dykes, referred to as the Dashigou swarm, are identified in the central and southeastern parts of the North China craton (NCC). They are 305–010° trending dykes, with widths of ~10–100 m and exposed lengths of several to >10 km. Precise U–Pb isotope dilution thermal ionization mass spectrometry (ID-TIMS) measurements on baddeleyite grains separated from three dykes yield ²⁰⁷Pb/²⁰⁶Pb average ages of 924.0 ± 3.7 Ma (Dashigou dyke), 921.8 ± 2.6 Ma (Yangjiaogou dyke) and 925.8 ± 1.7 Ma (Taohuagou dyke). Baddeleyite grains from a late-stage pegmatite vein in the Dashigou dyke were analyzed by secondary ion mass spectrometry (SIMS) methods. These yield a ²⁰⁷Pb/²⁰⁶Pb average age of 920.4 ± 5.7 Ma. The Dashigou dyke swarm exhibits an overall radiating geometry (the overall fan angle is about 60°), with a focal point located along the southern margin of the eastern NCC, where a large ca. 900 Ma sill swarm was previously recognized. The rift system hosting these slightly younger sills, named the Xu–Huai Rift System, could represent two breakup-parallel arms of a rift–rift–rift triple junction related to the initiation of the magma center that produced the Dashigou dykes. The sills have similar characteristics and could be cogenetic with the Dashigou dykes. The Dashigou dykes are coarse-grained, composed mainly of clinopyroxene and plagioclase feldspar, with or without olivine. One of the most primitive dykes has 47.79 wt.% SiO₂, 6.41 wt.% MgO, 1.38 wt.% TiO₂, 17.77 wt.% Al₂O₃, 10.47 wt.% CaO and 0.62 wt.% K₂O. It shows slight enrichment in light rare earth elements and a slightly positive Eu/Eu* anomaly (1.1), and is slightly depleted in high field-strength elements compared to neighboring elements on a primitive mantle-normalized spidergram. The Dashigou dykes show some similarities with enriched-mid ocean ridge basalts (E-MORB) or ocean island basalts (OIB) and have εNd_t values of +1.8 to +3.1 and ⁸⁷Sr/⁸⁶Sr_t values of 0.7019–0.7047 (t = 920 Ma). All these characteristics indicate that they are not likely derived from the ancient lithospheric mantle under the NCC, but rather from a mantle source below, in the asthenosphere. This 925–900 Ma magmatism represents a second sub-lithospheric mantle upwelling event following the 1780–1730 Ma event that occurred shortly (~70 Ma) after the formation of the subcontinental lithospheric mantle (SCLM). Therefore the SCLM of the NCC was multiply metasomatized during asthenospheric upwellings (at least at 1780–1730 and 925–900 Ma), before most of its eastern part was finally removed during the Mesozoic. Collectively, these ~925 Ma dykes and ~900 Ma sills constitute a large igneous province (LIP) with an areal extent of about 0.5 Mkm² and a diameter of about 1000 km. This LIP probably resulted from a Neoproterozoic mantle plume centered along the present southern margin of the eastern NCC, and probably resulted in the break-off and rifting away of a separate crustal block. We speculate that this conjugate block could have been the combined São Francisco–Congo craton on the basis of precisely matched ages for the Bahia dykes (São Francisco craton) and Gangila–Mayumbian volcanic associations (western part of the Congo craton).

© 2011 Elsevier B.V. All rights reserved.

1. Introduction

The North China craton (NCC) (Fig. 1), one of the oldest cratons with a crustal record back to 3.8 Ga (e.g., Liu et al., 1992, 2008; Wu et al., 2008a), was finally cratonized during the late Paleoproterozoic (1900–

1850 Ma) (Guo et al., 2005; Kröner et al., 2005, 2006; Kusky and Li, 2003; Kusky et al., 2001, 2007; Li et al., 2000, 2002; Liu et al., 2005a, 2006a; Wilde et al., 2002; Zhai and Liu, 2003; Zhai and Santosh, 2011; Zhai et al., 2005, 2007; Zhao et al., 1998, 2001, 2005), as indicated, for instance, by the craton-scale giant 1780–1770 Ma Taihang mafic dyke swarm (Peng, 2010 and reference therein). It is revealed that the ancient (>1800 Ma) subcontinental lithospheric mantle (SCLM) of the NCC was still attached beneath the NCC till Paleozoic time, as indicated by mantle xenoliths from volcanics (e.g., Gao et al., 2002). After ca. 1800 Ma, a few

* Corresponding author. Tel.: +86 10 82998530.

E-mail address: pengpengwj@mail.iggcas.ac.cn (P. Peng).

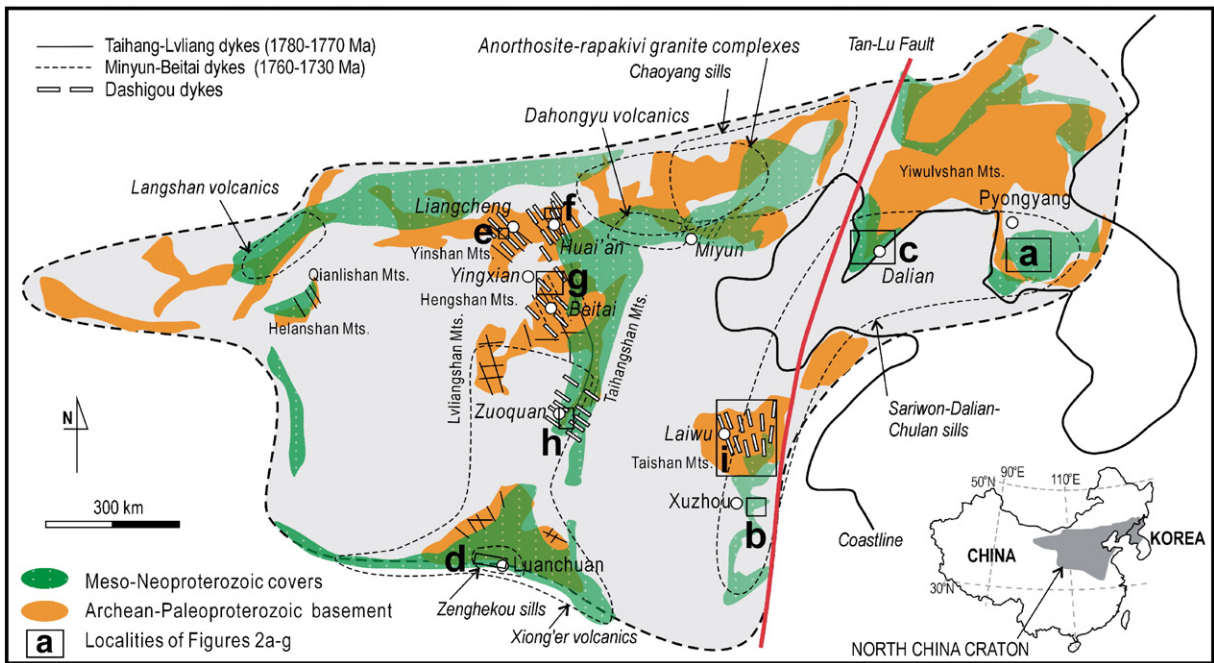


Fig. 1. Distribution of Precambrian dykes, sills and volcanics in the North China craton (1800–542 Ma). Letters a–h locate the maps of Fig. 2. See text for data sources.

magmatic events are reported and it was known that two important events affected the SCLM during early Mesozoic, i.e., 1) its northern and southern margins were possibly modified as a result from orogenic processes (e.g., Ernst et al., 2007; Miao et al., 2008; Xiao et al., 2003; Ye et al., 2000, 2009; Zhang et al., 2009a,b), and 2) its eastern part was mobilized, accompanied by destruction and thinning, predominantly around 120 Ma (e.g., Davis et al., 2001; Gao et al., 2004; Menzies et al., 1993, 2007; Rudnick et al., 2004; Wilde et al., 2003; Wu et al., 2008b; Yang et al., 2008; Zhang et al., 2002).

In this paper, mafic dykes having ages of ~925 Ma are identified for the first time. Together with some ~900 Ma sills reported on earlier (Peng et al., 2011a), the distribution and geometry of these mafic magmatic units, as well as their petrogenesis, are investigated. Mafic dykes are usually derived from the mantle and using geochemistry we can trace back their evolution through time (e.g., Hanski et al., 2006). In this paper, we consider the implications, not only for regional geology and global correlations, but also for evolution of the SCLM below the NCC.

2. Geological background

Several generations of Precambrian mafic dykes/sills and related magmatic associations have been emplaced into NCC crust after its final consolidation at ca. 1850 Ma (Fig. 1): 1) the 1780–1770 Ma Taihang and Lvliang dykes and 1760–1730 Ma Miyun–Beitai dykes, mainly in the central but also other parts of the NCC, as well as the ca. 1780 Ma Xiong'er volcanics along the southern margin of the craton (Peng, 2010 and reference therein; Peng et al., 2011b); 2) a 1730–1620 Ma anorogenic anorthosite–rapakivi granite–high potassium volcanic suite in the central part of the northern margin (e.g. Li et al., 1995; Lu and Li, 1991; Lu et al., 2008; Ramö et al., 1995; Yu et al., 1996; Zhang et al., 2007; Zhao et al., 2004, 2009); 3) ca. 1350–1320 Ma mafic sills in the central-eastern part of the northern margin (Li et al., 2009; Zhang et al., 2009c); 4) ca. 900 Ma mafic sills in the eastern end of the southern margin (Chulan–Dalian–Sariwon (CDS) sills) (Peng et al., 2011a); and 5) ca. 860–800 Ma volcanics at the western end of the northern margin of the NCC (Peng et al., 2010).

2.1. Taihang–Lvliang–Miyun–Beitai dykes and Xiong'er volcanics (ca. 1780 Ma)

The 1780–1770 Ma giant radiating Taihang dyke swarm and the coeval cross-cutting Lvliang swarm and the subsequent 1760–1730 Ma Miyun–Beitai swarms are mainly distributed in the central and western parts of the NCC, as well as locally extending into its eastern parts (Peng, 2010 and reference therein; Peng et al., 2011b) (Fig. 1). Estimated outcrop area and magma volume are $>0.1 \text{ Mkm}^2$ and $>0.1 \text{ Mkm}^3$, respectively. However, counting the area covered with Quaternary sediments, the estimated extent area would be $>>0.3 \text{ Mkm}^2$. The dykes have widths mostly from 10 to 40 m, but some being up to 100 m, and with lengths up to several tens of kilometers. They are composed of gabbro to diabase, with a mineral assemblage of mainly plagioclase and clinopyroxene and accessory hornblende, titanomagnetite, with or without K-feldspar, biotite, and olivine or quartz. The Xiong'er volcanics were emplaced around 1780 Ma (Cui et al., 2011; He et al., 2009; Zhao et al., 2002). It has been shown that the Taihang and Lvliang dykes and most of the Xiong'er volcanics probably originated from the lithospheric mantle (e.g., Wang et al., 2004; Peng et al., 2007, 2008); whereas the Miyun–Beitai dykes are possibly of asthenosphere origin, or from a plume source (Peng et al., 2007, 2011b).

2.2. Anorthosite–rapakivi granite complexes (1730–1680 Ma) and high-potassium volcanics (1620 Ma)

Anorthosite–rapakivi granite complexes occur as a number of small plutons or stocks. One of the larger of these plutons includes the Damiao Anorthosite Complex with an outcrop area of about 50 km^2 and the Shachang Rapakivi Complex covering about 25 km^2 (Ramö et al., 1995; Xie, 2005; Yang et al., 2005; Yu et al., 1996; Zhang et al., 2007; Zhao et al., 2004, 2009). Some ca. 1620 Ma high-potassium volcanics and some related sills are distributed mainly in the Dahongyu Formation of the Changcheng Group in the same area (Hu et al., 2007; Li et al., 1995; Lu and Li, 1991; Lu et al., 2008). They are thought to be derived either from the SCLM (e.g., Hu et al., 2007; Xie, 2005; Zhang et al., 2007) or from the crust (e.g., Ramö et al., 1995; Yang et al., 2005; Zhao et al., 2009).

2.3. Chaoyang mafic sills (1350–1320 Ma)

These sills are distributed in eastern Hebei (Li et al., 2009) and western Liaoning provinces (Zhang et al., 2009c) at the eastern end of the northern margin of the NCC. These sills are several meters to 100 m in thickness and intrude into Mesoproterozoic strata. The rocks are diabasic and have a mineral assemblage of pyroxene and plagioclase, with minor magnetite and hornblende. The rocks have experienced different degrees of alteration. Baddeleyite and zircon U–Pb ages from 1353 Ma to 1320 Ma have been reported (Li et al., 2009; Zhang et al., 2009c).

2.4. Chulan–Dalian–Sariwon (CDS) sills (900 Ma)

These sills are distributed along the southeastern margin of the NCC, i.e., Korean (Pyongnam basin, Fig. 2a), Shandong (Xu–Huai area, Fig. 2b), and Liaodong (Dalian area, Fig. 2c) peninsulas (e.g., 899 ± 7 Ma, baddeleyite $^{207}\text{Pb}/^{206}\text{Pb}$ age for a Sariwon sill, Peng et al., 2011a), as well as in the Luanchuan area (Zenghekou) of the western Henan Province (Yan et al., 2010) (Fig. 2d). Individual sills are meters to 150 m in thickness and extend for kilometers. The rocks are typical diabase, metamorphosed up to greenschist facies, and are composed of primary clinopyroxene and feldspar (present as relics) along with metamorphic minerals of epidotite, chlorite, Na-rich plagioclase and hornblende. They have been slightly deformed and share a consistent lineation with the country rocks. The metamorphism and deformation could have occurred at ca. 400 Ma resulting from an orogenic process affecting the cratonic margin (Peng et al., 2011a).

3. Occurrences and petrography

The dykes of this study are distributed in the central and southeastern parts of the NCC, e.g., Liangcheng (e.g., the Taohuagou dyke; Fig. 2e); Huai'an (e.g., the Yangjiaogou dyke, Fig. 2f), Hengshan Mountains (e.g., the Dashigou dyke; Fig. 2g), Zuoquan (Fig. 2h) and Laiwu–Yishui area (e.g., the Fengjiajuan dyke; Fig. 2i). They are typically 10–50 m (up to ~100 m) in width, and up to 10–20 km in length. Their trends vary from ~305–340° (central NCC), to ~010° (southeastern NCC) (Fig. 2e–i).

The 305–340°-trending dykes in the central NCC were previously considered to mostly belong to the 1780–1770 Ma Taihang swarm (e.g., Halls et al., 2000; Hou et al., 2008; Peng et al., 2004; Wang et al., 2008). However, there are also indicators that some of the dykes are younger. For example, in the Zuoquan area, the dykes cut the Mesoproterozoic sediments but are covered by Cambrian rocks (Fig. 2h).

In Laiwu–Yishui area, southeastern NCC, the 340–010°-trending dykes were also thought to be ca. 1800 Ma dykes (Hou et al., 2008; Wang et al., 2008); however, zircon ages as young as ca. 1000 Ma in a dyke from Laiwu County are reported by Hou et al. (2005). Thus some of these dykes should be no older than ca. 1000 Ma, and more exactly, they should be Neoproterozoic as some of them were unconformably covered by Cambrian strata. However, their relationship with the Neoproterozoic strata in this area, the Tumen Group, is unclear. The Tumen Group is thought to be comparable with those Neoproterozoic strata in the Xu–Huai basin, where ca. 900 Ma sills are identified (e.g., BGMRA, 1985; Liu et al., 2006b; Peng et al., 2011a).

The rocks comprise gabbro to diabase, are unmetamorphosed, and have a typical mineral assemblages of clinopyroxene (~25 vol.%) and plagioclase (~65 vol.%), and minor amounts of hornblende, biotite, K-feldspar, and magnetite, with or without olivine or quartz. Notably,

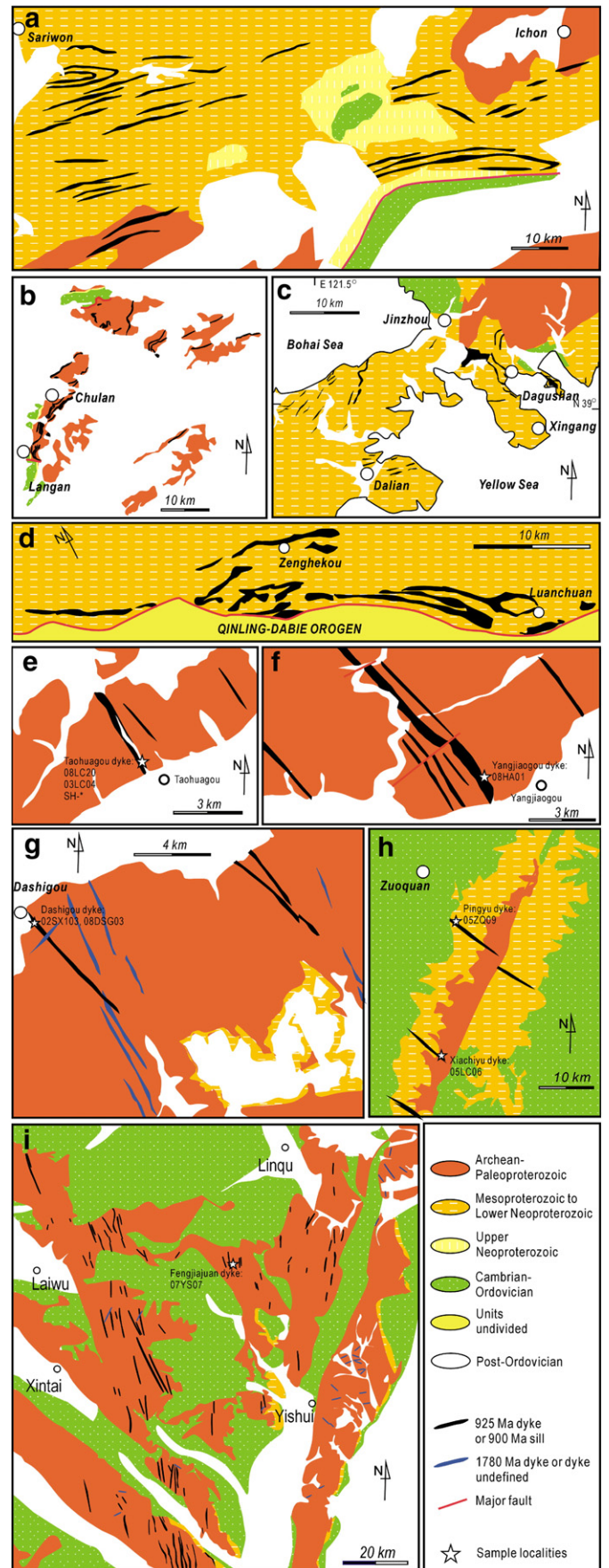


Fig. 2. Selected maps showing the distribution of 925–900 Ma mafic dykes and sills in the North China craton. a) sills in Sariwon area; b) sills in Xu–Huai area (Chulan); c) sills in Dalian area; d) sills in Luanchuan area (Zenghekou); e) dykes in Liangcheng area; f) dykes in Huai'an area; g) dykes in Yingxian area (Hengshan Mts.) (Dashigou); h) dykes in Zuoquan area (Southern Taihang Mts.); i) dykes in Laiwu–Yishui area; See Fig. 1 for localities of these maps in the North China craton.

the Yangjiaogou dyke from Huai'an area has a greater amount of olivine (~5–10 vol.%), with less plagioclase, and the dykes in Zuoquan area generally contain some K-feldspar in the mineral assemblage. There are also pegmatite veins in some of these dykes, with a common mineral assemblage of albite, quartz, hornblende and biotite.

4. Analytical methods

Samples for baddeleyite separation were collected from the coarse-grained parts of the dykes with one exception (08DSG03), which is from the pegmatite vein in a dyke. Baddeleyite grains were obtained using water-based separation techniques, with some of them performed on a *Wilfley* table at Lund University in Sweden following the method of *Söderlund and Johansson (2002)*. Fig. 3a–g show images of the baddeleyite and zircon grains using transmitted light, cathodoluminescence or backscatter electrons.

Isotope dilution thermal ionization mass spectrometry (ID-TIMS) was applied on baddeleyite grains in the geochronology lab of the Geological Survey of Canada. Twenty to thirty grains were grouped as a fraction, and the weight of each fraction was estimated using a digital weighing program (*Matthews and Davis, 1999*). Each fraction was first washed by 3 N HNO₃ and spiked with a ²⁰⁵Pb–²³³U–²³⁵U spike. A mixture of 48% HF and 16 N HNO₃ (10:1 by volume) was used to digest the fractions at 240–245 °C in *Teflon* containers inside metal bombs (dissolution vessels). After dissolution, the HF was evaporated and 3.1 N HCl was added to the samples which were then heated in the oven at 210 °C. The samples were then loaded onto columns and Pb and U were separated and dried down. Pb and U were loaded directly onto Re filaments with silica gel and then analyzed on a *Triton TI* mass spectrometer. Analytical results, calculated using in-house software (after *Davis, 1982*), are presented in *Table 1*. Ages were calculated

using *Isoplot (Ludwig, 2003)*. Analytical techniques were modified after *Roddick et al. (1987)* and *Parrish (1987)*.

Baddeleyite grains from sample 08DSG03 and a few zircon grains from sample 02SX103 were mounted in an epoxy resin and their Pb isotopic ratios were analyzed using a multi-collector *CAMECA 1280 IMS* machine with oxygen flooding technique in the State Key Laboratory of Lithospheric Evolution (Beijing) (SKLLE). The diameter of the analytical ion beam at the sample surface was approximately 20 μm. During data processing, the common Pb was assumed to be very low in the baddeleyites, and an average of present-day crustal composition (*Stacey and Kramers, 1975*) is used for the common Pb assuming that the common Pb is largely surface contamination introduced during sample preparation. The weighted means are given with 2-sigma errors. Analytical procedures and data processing were similar to those described in *Li et al. (2010)*.

Whole-rock chemical analyses were completed in the SKLLE, using samples mostly from the chilled margins of the dykes. Major element determinations were performed by X-ray fluorescence (*Shimadzu XRF-1700/1500*) after fusion with lithium tetraborate using Chinese national standard sample GBW07101-07114. The precision was better than 0.2 wt.% in the analysis range. The loss on ignition was measured as the weight loss of the samples after one hour of baking under a constant temperature at 1000 °C. Trace element analyses were determined using an *ELEMENT ICP-MS* after HNO₃ + HF digestion of about 40 mg of sample powder in a *Teflon* vessel, with accuracy and reproducibility monitored using Chinese national standard samples *GSR1* (granite), *GSR2* (rhyolite) and *GSR3* (basalt). The relative standard deviation was better than 5% above the detection limits.

Whole-rock Sr–Nd isotope determinations were performed on selected samples using a *Finnigan MAT 262* mass spectrometer in the SKLLE. *NBS 987* and *Ames* were used as references. During the analytical

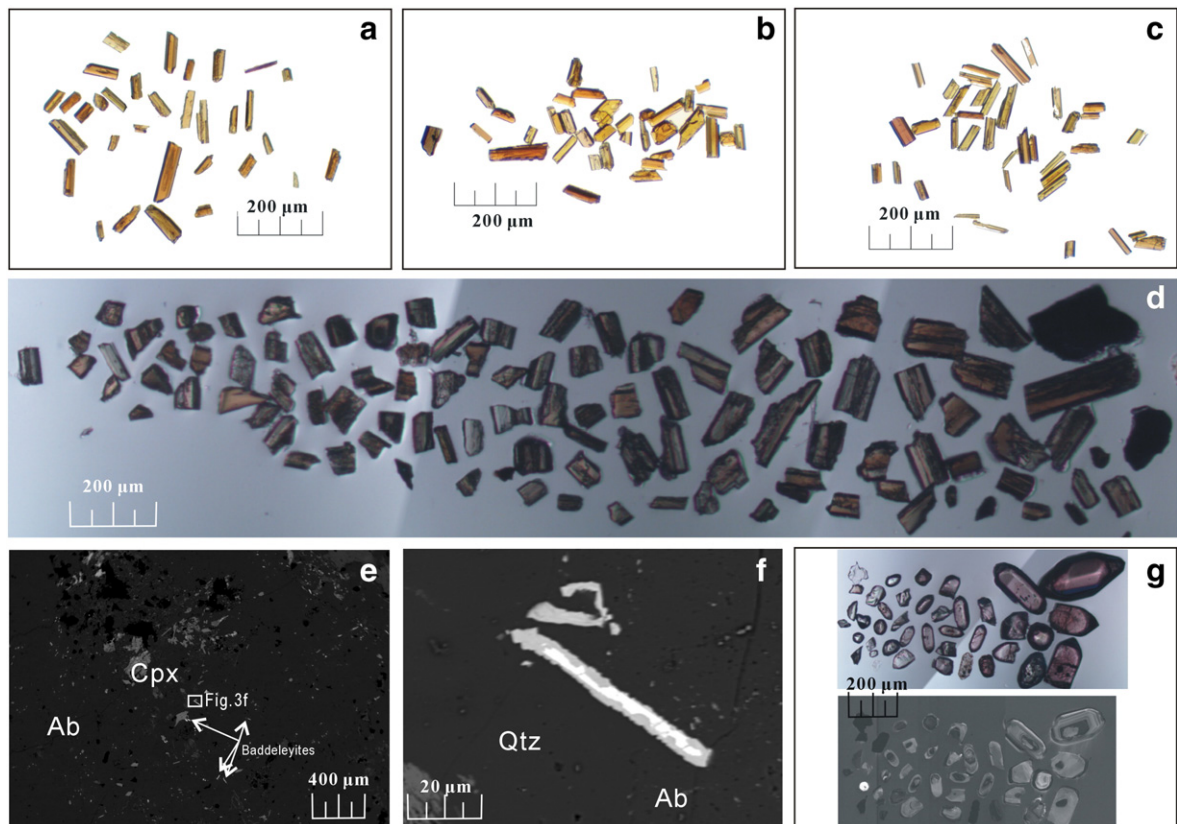


Fig. 3. Representative transmitted-light (TS), cathodoluminescence (CL) and backscatter-electron (BSE) images for zircon and baddeleyite grains of different samples: a) baddeleyite grains from sample 02SX103 (Dashigou dyke; TS); b) baddeleyite grains from sample 08HA01 (Yangjiaogou dyke; TS); c) baddeleyite grains from sample 08LC20 (Taohuagou dyke; TS); d) baddeleyite grains from sample 08DSG03 (Dashigou dyke; TS); e) and f) baddeleyite grains with zircon replacement, in thin section of 08DSG03 (Dashigou dyke; BSE); g) zircon grains from sample 02SX103 (Dashigou dyke; TS [upper] and CL).

Table 1
U–Pb analytical data.

A. ID-TIMS data																				
Fraction	Weight μg	U ppm	Pb ¹ ppm	²⁰⁶ Pb/ ²⁰⁴ Pb ²	Pb ³ pg	²⁰⁸ Pb/ ²⁰⁶ Pb ⁴	²⁰⁷ Pb/ ²³⁵ U ⁴	± 1σ	²⁰⁶ Pb/ ²³⁸ U ⁴	± 1σ	Corr coef ⁵	²⁰⁷ Pb/ ²⁰⁶ Pb ⁴	± 1σ	²⁰⁶ Pb/ ²³⁸ U ⁶	± 2σ	²⁰⁷ Pb/ ²³⁵ U ⁶	± 2σ	²⁰⁷ Pb/ ²⁰⁶ Pb ⁶	± 2σ	%disc ⁷
<i>02SX103</i>																				
B1	3.0	647	92	8822	2	0.030	1.445	0.0020	0.1502	0.00017	0.91	0.06979	0.00004	902.0	1.9	907.9	1.6	922.3	2.3	2.4
B2	3.0	646	87	2646	5	0.030	1.360	0.0019	0.1414	0.00014	0.85	0.06975	0.00005	852.7	1.6	871.9	1.6	920.9	3.0	7.9
B3	3.0	488	70	8456	2	0.030	1.465	0.0019	0.1520	0.00016	0.92	0.06989	0.00004	912.2	1.7	916.0	1.5	925.2	2.2	1.5
B4	3.0	680	96	7144	3	0.020	1.446	0.0020	0.1500	0.00017	0.92	0.06993	0.00004	900.9	1.9	908.2	1.6	926.2	2.3	2.9
<i>08HA01</i>																				
B1	9.0	63	9	187	30	0.030	1.46	0.013	0.1515	0.00039	0.70	0.06982	0.00053	909.6	4.3	913.6	11.0	923.2	30.8	1.6
B2	4.0	204	30	484	14	0.040	1.468	0.0052	0.1523	0.00020	0.70	0.06993	0.00019	913.8	2.3	917.5	4.2	926.3	11.3	1.4
B3	3.0	427	61	2103	5	0.030	1.458	0.0020	0.1516	0.00014	0.85	0.06975	0.00005	910.1	1.5	913.3	1.7	920.9	3.2	1.3
B4	2.0	177	25	1314	3	0.030	1.454	0.0025	0.1510	0.00019	0.70	0.06983	0.00009	906.7	2.1	911.6	2.1	923.2	5.1	1.9
<i>08LC20</i>																				
B1	3.0	655	93	6350	3	0.020	1.460	0.0019	0.1515	0.00016	0.92	0.06990	0.00004	909.2	1.8	913.9	1.6	925.4	2.2	1.9
B2	3.0	138	19	750	5	0.020	1.459	0.0037	0.1513	0.00018	0.68	0.06990	0.00013	908.4	2.0	913.4	3.0	925.5	7.8	2.0
B3	3.0	147	21	409	9	0.030	1.466	0.0058	0.1519	0.00020	0.69	0.07001	0.00022	911.4	2.3	916.5	4.8	928.7	13.0	2.0
B4	3.0	230	32	3870	1	0.020	1.459	0.0020	0.1513	0.00015	0.85	0.06993	0.00005	908.4	1.7	913.6	1.6	926.3	2.9	2.1
B. SIMS data																				
Grains	²⁰⁷ Pb/ ²⁰⁶ Pb ⁸		± 1σ%	²⁰⁴ Pb/ ²⁰⁶ Pb		± 1σ%	²⁰⁷ Pb/ ²⁰⁶ Pb ⁹		± 1σ%	²⁰⁷ Pb/ ²⁰⁶ Pb ages		± 2σ								
1	0.07062		0.34	3.7E-06		41	0.07057		0.34	945		14								
2	0.07056		0.48	7.3E-05		28	0.06955		0.64	915		27								
3	0.06979		0.38	5.2E-06		32	0.06972		0.38	920		16								
4	0.06996		0.24	1.4E-05		12	0.06975		0.25	921		10								
5	0.06949		0.25	8.1E-06		21	0.06938		0.25	910		11								
6	0.07002		0.22	1.4E-05		25	0.06982		0.23	923		9								
7	0.06935		0.27	5.4E-06		29	0.06928		0.28	907		11								
16	0.06969		0.28	5.1E-06		25	0.06961		0.28	917		12								
9	0.07040		0.35	4.6E-05		9.8	0.06975		0.37	921		15								
10	0.07219		0.41	1.7E-04		8.9	0.06972		0.53	920		22								
11	0.07062		0.45	2.3E-05		22	0.07030		0.46	937		19								
12	0.07061		0.49	2.7E-05		17	0.07023		0.50	935		21								
17	0.06981		0.45	4.4E-06		31	0.06975		0.45	921		19								
14	0.07028		0.65	6.0E-06		44	0.07019		0.65	934		27								
15	0.07086		0.31	9.9E-05		12	0.06945		0.40	912		16								

Note: 1. Radiogenic Pb; 2. Measured ratio, corrected for spike and fractionation; 3. Total common Pb in analysis corrected for fractionation and spike; 4. Corrected for blank Pb and U and common Pb, Pb blank isotopic composition is based on the analysis of procedural blanks, corrections for common Pb were made using Stacey-Kramers compositions (Stacey and Kramers, 1975); 5. Correlation coefficient; 6. Corrected for blank and common Pb. 7. Percent discordance. 8. Measured ratio; 9. Corrected for common Pb using Stacey-Kramers compositions (Stacey and Kramers, 1975).

period, they were 0.710238 ± 12 (2 SD, standard deviation) and 0.512138 ± 11 (2 SD), respectively. Standard material BCR-2 (basalt powder, $^{87}\text{Sr}/^{86}\text{Sr} = 0.705027 \pm 9$ (2 SD, $n = 10$), $^{143}\text{Nd}/^{144}\text{Nd} = 0.512645 \pm 11$ (2 SD, $n = 10$), data of this time) was processed with the selected samples to monitor the error of the procedure. Blanks for Rb–Sr and Sm–Nd isotope analyses were better than 100 and 50 pg, respectively. The external precisions (2σ) of $^{87}\text{Rb}/^{86}\text{Sr}$ and $^{147}\text{Sm}/^{144}\text{Nd}$ ratios were both better than 0.5%.

5. Age results

5.1. Samples 02SX103 (Dashigou dyke)

This sample is from the coarse grained part (~10 m from the margin) of a ~40 m-wide dyke, trending ~315°, in Dashigou village, Yingxian county (GPS: N39°28', E113°20'). Baddeleyite grains in this sample are light brownish to yellowish, lamellar and needle-like, and up to 150 μm long (Fig. 3a). There are thin rims of polycrystalline zircon on some of the baddeleyite grains. The four analyzed fractions have estimated weights of about 3.0 μg, U concentrations of 488–688 ppm, radiogenic Pb of 70–96 ppm, and common lead of 2–5 pg (Table 1). Fig. 4a is the concordia diagram for the four fractions, and the data show about 1.5–7.9% discordance. Sometimes, minor discordance of baddeleyite fractions during ID-TIMS analysis is due to the thin rims of polycrystalline

zircon or zirconolite as revealed by other studies; under such circumstance, $^{207}\text{Pb}/^{206}\text{Pb}$ ages are used as best estimation (e.g., Heaman and LeCheminant, 1993, 2001). The $^{207}\text{Pb}/^{206}\text{Pb}$ ages vary from 921 ± 3 Ma to 926 ± 2 Ma, with an average of 924.0 ± 3.7 Ma (2σ , $n = 4$, MSWD = 3.8) and an upper intercept age of $925.9 \pm 2.3/-2.0$ Ma (2σ , $n = 4$, MSWD = 2.8).

A few zircon grains (Fig. 3g) from sample 02SX103 were analyzed using the SIMS method on a CAMECA IMS 1280 machine, yielding ages of ca. 2500 Ma and 1800 Ma.

5.2. Sample 08HA01 (Yangjiaogou dyke)

This sample is from the coarse-grained part (~5 m from the margin) of a ~100 m-wide, 330–325° trending dyke sampled west of Yangjiaogou village, Huai'an county (GPS: N 40°44', E 114°07'). Baddeleyite grains from this sample are brownish, to yellowish, lamellar, and about 50–150 μm in their longest dimension (Fig. 3b). The four fractions selected for isotopic analysis have estimated weights of about 2.0–9.0 μg, U concentrations of 63–427 ppm, radiogenic Pb of 9–61 ppm, and common lead of 3–30 pg (Table 1). Fig. 4b is the concordia diagram for the four fractions, and shows 1.3–1.9% discordance. $^{207}\text{Pb}/^{206}\text{Pb}$ ages vary from 921 ± 3 Ma to 926 ± 11 Ma, with an average of 921.8 ± 2.6 Ma (2σ , $n = 4$, MSWD = 0.42). Regression yields an upper intercept age of 920 ± 12 Ma (2σ , $n = 4$, MSWD = 0.63).

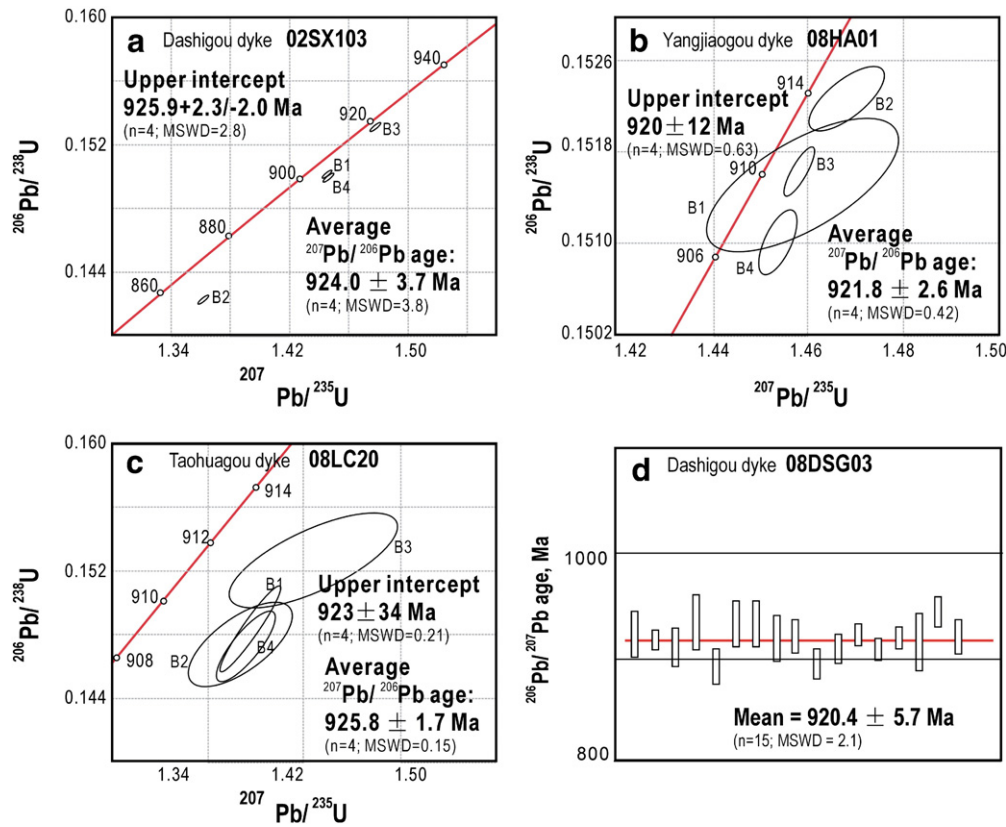


Fig. 4. Concordia U–Pb age diagrams and average Pb–Pb age plots: a) sample 02SX103 (Dashigou dyke); b) sample 08HA01 (Yangjiaogou dyke); c) sample 08LC20 (Taohuagou dyke); d) sample 08DSG03 (pegmatite vein in the Dashigou dyke).

5.3. Sample 08LC20 (Taohuagou dyke)

The sample is from the center of a ~30 m-wide, 325°-trending dyke located to the north of Taohuagou village, Liangcheng county (GPS: N40°31', E112°22'). Baddeleyite grains are brownish to yellowish, lamellar and needle-like and up to 150 μm long (Fig. 3c). The four analyzed fractions have estimated weights of about 3.0 μg, U concentrations of 147–655 ppm, radiogenic Pb of 19–93 ppm, and common lead of 1–9 pg (Table 1). Fig. 4c is the concordia diagram of the fractions, and it reveals that they have about 1.9–2.1% discordancy. Their $^{207}\text{Pb}/^{206}\text{Pb}$ ages vary from 925 ± 2 Ma to 929 ± 13 Ma. They give an average $^{207}\text{Pb}/^{206}\text{Pb}$ age of 925.8 ± 1.7 Ma (2σ , $n = 4$, MSWD = 0.15) and an upper intercept age of 923 ± 34 Ma (2σ , $n = 4$, MSWD = 0.21).

5.4. Sample 08DSG03 (pegmatite vein in Dashigou dyke)

This sample is from the pegmatite vein of the Dashigou dyke from the same locality as sample 02SX103. The pegmatite is composed mainly of albite and quartz with minor clinopyroxene (Fig. 3e, f). Baddeleyite grains from this sample are lamellar and needle-like, and mostly less than 200 μm long. A few grains show thin rims of polycrystalline zircon (Fig. 3d–f). Pb isotopic ratios of 15 grains were analyzed using a CAMECA IMS 1280 machine (Table 1). $^{207}\text{Pb}/^{206}\text{Pb}$ ratios range from 0.06935 to 0.07219 and $^{206}\text{Pb}/^{204}\text{Pb}$ ratios vary from 1.7×10^4 to 3.7×10^6 . The weighted average $^{207}\text{Pb}/^{206}\text{Pb}$ age is 920.4 ± 5.7 Ma (2σ , $n = 15$, MSWD = 2.1). This age is very close to the ID-TIMS age obtained from baddeleyite grains separated from coarse-grained diabase from the same site in this Dashigou dyke (Section 5.1).

6. Chemical results

Most samples of the studied dykes and the ~900 Ma sills are tholeiitic (Fig. 5a, b). The dykes from the Liangcheng and Hengshan area have

very consistent chemistry, i.e., they have SiO_2 of 50.71–52.63 wt.%, TiO_2 of 2.88–3.31 wt.%, Al_2O_3 of 12.82–14.80 wt.%, FeO_t (total iron) of 13.9–16.3 wt.%, MnO of 0.20–0.26 wt.%, MgO of 3.32–4.02 wt.%, CaO of 6.91–7.62 wt.%, Na_2O of 2.56–2.91 wt.%, K_2O of 1.50–2.12 wt.%, and P_2O_5 of 0.67–0.75 wt.% (Table 2). They have slight light rare earth element (REE) enrichment ($\text{La}/\text{Yb}_N = 1.97$ –2.38; Table 2) and negative Eu anomalies ($\text{Eu}/\text{Eu}^* = 0.70$ –0.82, $\text{Eu}/\text{Eu}^* = \text{Eu}_N / [(\text{Sm}_N)(\text{Gd}_N)]^{1/2}$) (Fig. 5c). They show slightly negative anomalies in high field-strength elements (HFSE, e.g., Nb, Ti) compared with the neighboring elements in multi-element spidergrams normalized to primitive mantle (after values given by Sun and McDonough, 1989) (Fig. 5d). They give consistent Nd and Sr isotopic ratios, i.e., the ϵNd_t values range from +1.8 to +3.1 (Fig. 6), and $^{87}\text{Sr}/^{86}\text{Sr}_t$ values range from 0.7019 to 0.7047 ($t = 920$ Ma; Table 2).

However, the Yangjiaogou dyke from Huai'an area (sample 08HA01) has distinctly higher MgO (6.41 wt.%), Al_2O_3 (17.77 wt.%), and CaO (10.47 wt.%) concentrations, but lower SiO_2 (47.79 wt.%), TiO_2 (1.38 wt.%), and K_2O (0.62 wt.%) (Table 2). This dyke shows slight light REE enrichment and a slightly positive Eu/Eu^* value (1.1) and little depletion in HFSE elements (Table 2; Fig. 5c, d).

The major element concentrations of the dykes from Zuoquan area match those of Taohuagou and Dashigou dykes, except for having slightly higher K_2O contents (up to 3.74 wt.%) (Table 2). They have more strongly differentiated REE patterns, e.g., $\text{La}/\text{Yb}_N = 4.47$ –4.7. In addition, they show positive anomalies in Eu ($\text{Eu}/\text{Eu}^* = \sim 1.1$).

The Fengjiajuan dyke from Laiwu area shows a similar composition to that of sample 08HA01, except that it has slightly greater SiO_2 , FeO_t , Rb, Ba, Th and K_2O contents but slightly lower CaO and Al_2O_3 (Fig. 5a–d; Table 2). Their $\text{La}/\text{Yb}_N = 1.59$ and $\text{Eu}/\text{Eu}^* = 1.1$ (slightly positive Eu anomalies) (Fig. 5c; Table 2).

The pegmatite vein in the Dashigou dyke (sample 08DSG03) is composed of mainly albite, quartz and clinopyroxene, and has a SiO_2 concentration of 67.87 wt.% and a Na_2O concentration of 8.53 wt.%. It

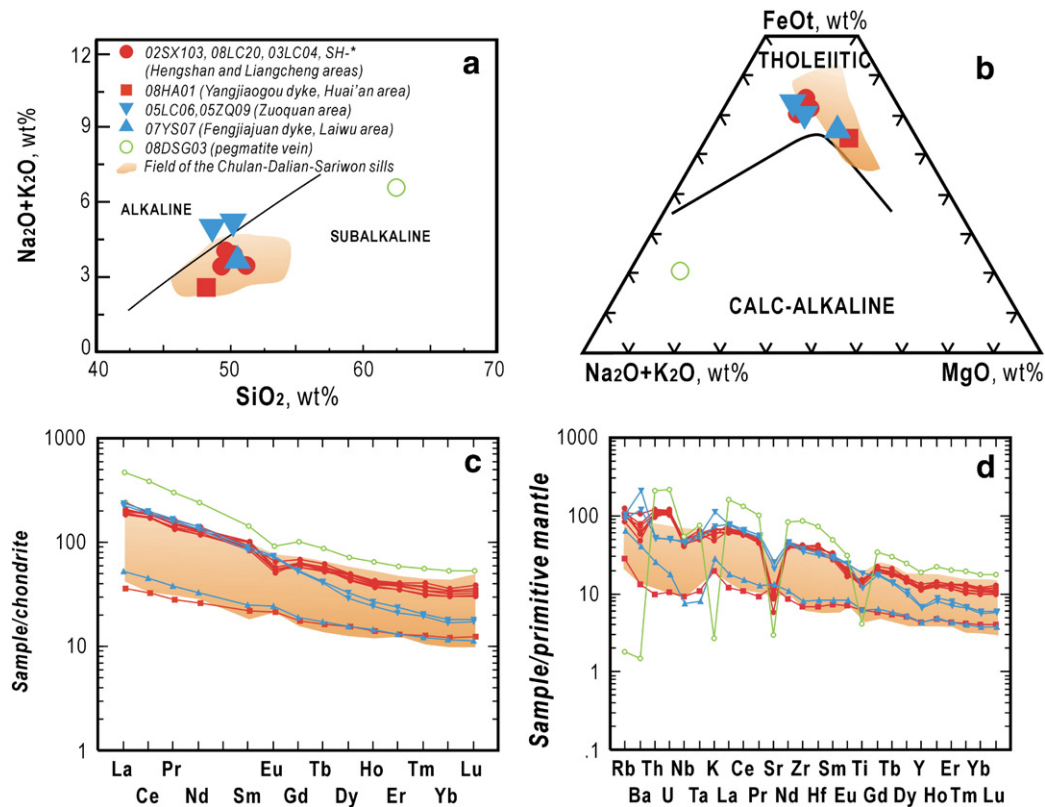


Fig. 5. a) Na₂O + K₂O vs. SiO₂ diagram (after Irvine and Baragar, 1971); b) FeO_t–Na₂O + K₂O–MgO ternary diagram (after Irvine and Baragar, 1971); c) Chondrite-normalized REE patterns; and d) primitive mantle-normalized trace element spidergram for the Dashigou dykes, as well as the Chulan–Dalian–Sariwon (CDS) sills (after Peng et al., 2011a and reference therein). Chondrite and primitive mantle-normalized values are after Sun and McDonough (1989).

shows a similar REE pattern to its host, the Dashigou dyke, but is extremely depleted in Rb, Ba, K, Sr and Ti concentrations on the spidergram (Fig. 5c, d). This is a highly differentiated composition possibly representing the latest stage differentiate of the Dashigou dyke.

7. Discussions

7.1. Geometry of the Dashigou dyke swarm

We suggest that all the studied dykes constitute a single swarm, herein labeled the Dashigou swarm. They also have similar petrographic characteristics and chemical compositions. Some of these dykes have orientations parallel to the older 1780 Ma dykes (Fig. 1); but they can be distinguished on the basis of different chemistry (Fig. 7). Baddeleyite ages reveal that the dated dykes are emplaced at 925.8–920.4 Ma, and the 12 fractions in Table 1A from the three dykes yield a ²⁰⁷Pb/²⁰⁶Pb average age of 924.2 ± 1.4 Ma (MSWD = 1.8).

Collectively, the dykes in Zuoquan (~305° trend), Yingxian (Hengshan Mts.) (~315°), Liangcheng (~325°), Huai'an (~330–325°) and Laiwu–Yishui (~340–010°) areas (Fig. 2e–i) show a clear radiating geometry (the overall fan angle is ~60°), with an apparent focal point located further southeast, close to the Chulan (Fig. 8a).

Fig. 8a is a simplified geological map with the offset resulting from strike slip along the Tan–Lu fault corrected (using the offset as estimated by Xu et al., 1987; Xu and Zhu, 1995). Based on this map, Peng et al. (2011a) noted that the 900 Ma sills in Shandong, Jiaodong and Korean Peninsulas (Xu–Huai, Lv–Da and Pyongnam Basins) constitute a related sill complex, named the Chulan–Dalian–Sariwon (CDS) sill swarm (or complex). We realize that the distribution of this sill swarm could be expanded further if the sills and volcanics of central Henan Province (Luanchuan Basin: north to the Qinling–Dabie Orogen, an orogen

between the NCC and South China craton; Fig. 2d) are also related, based on similar ages (800–900 Ma) as reported by Yan et al. (2010). These sills indeed have similar chemistry to the Dashigou dykes, e.g., REE and trace element patterns (Fig. 5a–d). The apparent magma center of the Dashigou swarm (based on the focus of the dyke swarm) was located close to Chulan, where ca. 900 Ma sills are identified.

The four basins hosting sills and volcanic rocks, the Xu–Huai, Lv–Da, Pyongnam, and Luanchuan basins, could constitute a Neoproterozoic rift system along the southeastern margin of the NCC; it is herein referred to as the Xu–Huai Rift System. This rift system has two branches (arms), along the southeastern and southern margins of the eastern NCC respectively, with an angle of about 120–140°. These could be part of a rift–rift–rift ‘triple junction’ (e.g., Dewey and Burke, 1973) with the third rift arm carried as an aulacogen in the formerly (as yet unidentified) conjugate crustal block. The focal point of the radiating Dashigou dyke swarm is associated with the center of this triple junction and suggests that a mantle plume initiated this triple junction rifting (see discussion of geochemistry below). Such a model would predict associated flood basalts, and possibly alkaline intrusions (e.g., Kumarapeli, 1993), particularly along the rift system. Together, the Dashigou dyke swarm and the Xu–Huai Rift System cover an area of about 0.5 Mkm² with a maximum extent of about 1000 km. This areal extent could be comparable to those of other large igneous provinces (LIPs) (e.g., Bryan and Ernst, 2008; Coffin and Eldholm, 1994).

7.2. Evidence for a mantle plume and implication for the evolution of the SCLM

The compositions of the ~925 Ma dykes and ~900 Ma sills are not primitive and are consistent with some fractionation, as well as assimilation/contamination (Figs. 5–7). The Yangjiaogou and

Table 2
Whole-rock major and trace element and Sr–Nd isotope data.

A. major (wt.%) and trace (ppm) element													
Sample	08DSG03	08HA01	02SX103	08LC20	03LC04	SH-12	SH-13	SH-14	SH-15	SH-16	05LC06	05ZQ09	07YS07
SiO ₂	67.87	47.79	52.63	50.71	51.41	51.84	52.07	51.88	51.61	52.19	50.20	48.69	50.67
TiO ₂	0.89	1.38	3.18	3.31	3.08	3.07	2.89	2.88	3.30	3.08	2.72	4.39	1.42
Al ₂ O ₃	16.00	17.77	12.92	12.96	13.34	13.71	14.78	14.80	12.82	13.36	14.47	14.24	14.68
FeO _t	3.0	12.7	15.7	16.3	15.9	14.8	13.9	14.0	15.3	15.0	16.3	15.4	13.8
MnO	0.04	0.15	0.26	0.21	0.20	0.25	0.25	0.23	0.25	0.24	0.25	0.18	0.19
MgO	1.29	6.41	3.44	3.83	3.63	3.72	3.32	3.37	4.02	3.59	3.19	3.99	6.40
CaO	2.16	10.47	6.91	6.96	6.91	7.19	7.33	7.39	7.62	7.14	6.59	7.02	8.88
Na ₂ O	8.53	2.52	2.56	2.83	2.85	2.77	2.89	2.91	2.88	2.64	3.10	1.46	2.87
K ₂ O	0.08	0.62	1.70	2.12	2.02	2.00	1.87	1.92	1.50	2.09	2.31	3.74	0.88
P ₂ O ₅	0.19	0.13	0.68	0.75	0.70	0.70	0.65	0.66	0.75	0.71	0.89	0.93	0.18
LOI	1.28	2.46	2.04	1.45	1.70	3.29	3.42	3.65	3.60	3.46	2.6	5.68	1.22
Mg#	54	57	36	38	37	40	38	39	41	39	34	40	52
Rb	1.13	18.1	61.0	79.5	67.5	69.1	66.6	64.6	52.5	69.9	68.8	60.1	42.4
Sr	61.2	266	212	196	182	206	220	220	124	202	553	455	291
Ba	10.2	93.0	519	405	443	544	404	423	334	729	1545	885	295
Th	17.3	0.83	8.91	8.05	8.43	10.0	9.33	8.82	9.72	10.4	4.45	4.68	2.27
U	4.49	0.22	2.23	2.28	2.52	2.38	2.19	2.16	2.29	2.47	1.11	1.08	0.39
Pb	1.82	1.91	27.0	12.2	10.9	14.9	12.5	12.4	10.3	16.7	19.7	17.4	5.44
Zr	940	75.7	461	428	449	463	440	431	453	468	436	402	93.3
Hf	22.3	2.15	13.2	10.2	11.0	12.0	11.2	11.2	11.6	12.2	10.7	9.97	2.64
Nb	37.8	6.67	35.8	30.0	29.2	34.3	31.4	32.2	35.7	35.1	33.5	35.8	5.53
Ta	3.03	0.45	2.65	2.36	2.29	2.06	2.11	2.11	2.36	2.34	2.27	2.47	0.34
Sc	12.6	30.1	30.1	–	–	28.4	25.5	25.1	30.1	26.4	14.2	16.8	32.9
V	30.5	222	246	–	–	280	260	251	303	267	201	300	288
Cr	11.4	91.9	40.3	32.7	34.1	50.3	40.4	41.8	51.5	46.4	6.49	47.4	214
Co	6.83	54.5	34.0	28.4	29.5	36.9	35.3	34.2	39.1	36.1	35.7	38.7	47.4
Ni	2.57	96.9	13.8	11.6	12.3	16.0	14.1	13.3	16.2	14.8	20.0	39.7	45.9
Cu	23.8	58.6	26.2	33.0	32.4	28.1	27.3	28.5	25.1	30.0	54.6	64.1	51.2
Be	1.43	0.53	2.90	–	–	3.00	2.77	2.70	3.20	2.86	2.48	1.87	0.74
Ga	21.5	20.8	28.0	23.7	25.1	26.4	26.0	25.6	26.7	26.1	26.8	24.2	20.3
Cs	0.29	1.41	4.29	3.45	1.44	1.62	2.79	2.06	1.42	1.97	1.02	1.07	0.82
La	108	8.20	54.4	43.9	46.9	46.7	43.3	42.0	44.9	45.4	56.2	53.7	12.6
Ce	226	19.1	112	101	107	111	102	99.9	109	109	122	116	27.4
Pr	27.6	2.54	14.8	12.8	13.4	13.6	12.6	12.3	13.6	13.4	15.9	15.2	3.61
Nd	109	11.7	62.9	56.1	57.7	56.9	53.2	53.4	59.4	57.5	65.6	62.3	15.4
Sm	21.3	3.26	13.4	12.1	13.0	14.6	12.8	13.2	14.8	14.4	13.7	12.8	3.85
Eu	5.13	1.20	3.59	2.84	3.00	3.06	3.08	3.04	3.20	3.05	4.34	4.23	1.43
Gd	20.1	3.46	13.5	12.5	12.6	12.0	11.4	11.5	12.6	12.3	11.1	10.8	3.93
Tb	3.14	0.59	2.24	1.98	1.98	2.02	1.86	1.92	2.08	1.91	1.57	1.52	0.65
Dy	17.6	3.79	12.0	10.5	10.7	11.9	11.3	11.3	12.1	11.9	8.25	7.41	3.95
Ho	3.55	0.77	2.32	2.02	2.03	2.19	2.08	2.14	2.32	2.29	1.52	1.37	0.83
Er	9.40	2.08	6.44	5.58	5.63	6.13	6.15	6.03	6.34	6.36	3.95	3.50	2.17
Tm	1.39	0.31	0.99	0.75	0.77	0.84	0.84	0.83	0.94	0.91	0.52	0.50	0.31
Yb	8.63	1.97	5.94	4.89	4.88	5.41	5.23	5.25	5.64	5.56	3.11	2.83	1.96
Lu	1.29	0.30	0.94	0.73	0.75	0.84	0.79	0.80	0.88	0.88	0.46	0.44	0.29
Y	83.6	19.5	60.5	50.5	51.0	53.1	51.3	50.7	54.4	52.3	32.5	31.5	20.4
REE	47.0	78.7	312	275	284	340	318	314	342	338	341	324	98.7
La/Yb _N	3.10	1.03	2.27	2.22	2.38	2.14	2.05	1.98	1.97	2.02	4.47	4.70	1.59
Gd/Yb _N	1.93	1.46	1.97	2.25	2.19	1.83	1.81	1.81	1.85	1.83	2.94	3.15	1.66
Eu/Eu*	0.76	1.09	0.71	0.82	0.72	0.71	0.78	0.76	0.72	0.70	1.08	1.10	1.12

B. Sr–Nd isotopes																
Samples	Rb ppm	Sr ppm	⁸⁷ Rb/ ⁸⁶ Sr	⁸⁷ Sr/ ⁸⁶ Sr	2σ	⁸⁷ Sr/ ⁸⁶ Sr _i	2σ	Sm ppm	Nd ppm	¹⁴⁷ Sm/ ¹⁴⁴ Nd	¹⁴³ Nd/ ¹⁴⁴ Nd	2σ	εNd _t	2σ	fSm/Nd	TDM Ga
02SX103	59.08	194.15	0.8780	0.716247	0.000011	0.7047	0.0018	13.00	56.71	0.1388	0.512445	0.000011	3.1	0.9	–0.29	1.4
03LC03	70.76	157.17	1.2934	0.718906	0.000009	0.7019	0.0026	12.35	53.65	0.1393	0.512437	0.000009	2.8	0.8	–0.29	1.5
SH-12								12.06	53.83	0.1355	0.512377	0.000005	2.1	0.8	–0.31	1.5
SH-13								11.67	50.90	0.1386	0.512399	0.000008	2.2	0.8	–0.30	1.5
SH-14								10.55	47.03	0.1357	0.512384	0.000007	2.2	0.8	–0.31	1.5
SH-15								11.41	49.86	0.1384	0.512376	0.000005	1.8	0.8	–0.30	1.6
SH-16								12.83	56.61	0.1370	0.512405	0.000008	2.5	0.8	–0.30	1.5

Note: 1.Total major element concentrations are normalized to 100 wt.%. 2. FeO_t = total iron; 3.LOI = Loss On Ignition; 4.Mg# = Mg numbers, Eu/Eu* = Eu anomalies, see text for detail; 5. La/Yb_N and Gd/Yb_N values are normalized to chondrite after Sun and McDonough (1989). 6. Initial Sr–Nd isotopic ratios are calculated back to 920 Ma.

Fengjiajuan dykes (samples 08HA01 and 07YS03) have the highest MgO content (~6.4 wt.%) and show the least differentiated compositions among the analyzed dykes. Most others show a strong depletion in Sr contents, negative Eu anomalies and strong LREE enrichment (La/Yb_N value up to 4.70; Table 2), possibly resulting

from feldspar (plagioclase) fractionation. Their depleted HFSE concentrations could result from crustal assimilation/contamination. In general, the trace element patterns of the 925–900 Ma dykes and sills varied from E-MORB to OIB on a primitive-mantle normalized spidergram (Figs. 5d and 6).

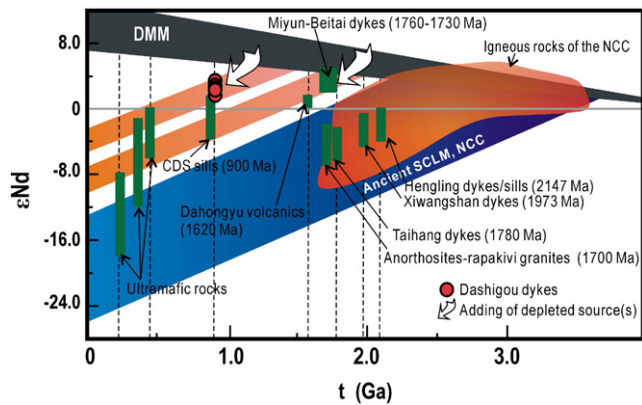


Fig. 6. ϵ_{Nd} vs. time (t , Ga) diagram for the 925–900 Ma mafic dykes and sills in the North China craton (NCC) and comparison with other associations. Data of “igneous rocks of the NCC” are from Wu et al. (2005); data of Hengling dykes/sills (2147 Ma) and Xiwangshan dykes (1973 Ma) are from Peng (2005); data of Taihang dykes (ca. 1780 Ma) are from Peng et al. (2007); data of Miyun-Beitai dykes (1760–1730 Ma) are from Peng et al. (2011b); data of anorthosite-rapakivi granite associations (1700 Ma) are from Ramö et al. (1995), Xie (2005) and Zhao et al. (2009); data of Dahongyu volcanics (1620 Ma) are from Hu et al. (2007); data of CDS sills (900 Ma) are from Peng et al. (2011a); and data of “ultramafic rocks” from the northern margin of the NCC are from Zhang et al. (2009a). DMM = depleted MORB mantle; SCLM = sub-continental lithospheric mantle.

The Dashigou dykes and CDS sills have chemical characteristics distinct from the 1780–1770 Ma Taihang dykes (the major pulse of this 1780–1730 Ma LIP) and the Xiong'er volcanics (Peng, 2010 and reference therein), which are similar to those derived from the ancient lithospheric mantle of the NCC (e.g., Wang et al., 2004; Peng et al., 2008) (Fig. 7). However, these 925–900 Ma dykes/sills have some similarities to the later phase of this earlier LIP, the 1760–1730 Ma Miyun-Beitai dykes, which are thought to be derived from asthenosphere (Peng et al., 2007, 2011b) (Fig. 7). So it is possible that these Neoproterozoic dykes and sills originated from the altered domain(s) of the SCLM of the NCC, which were metasomatized during the earlier 1760–1730 Ma magmatism. This effect is apparently stronger for the CDS sills, but less significant for the Dashigou dykes, which have more depleted Nd isotopes (Fig. 7). We propose that a depleted source component, likely the asthenosphere or mantle below, has contributed to the evolution of the 925 Ma LIP, and that metasomatized lithosphere possibly affect some units, particularly the sills more so than the dykes.

The large areal extent of the Dashigou dykes/CDS sills (and interpreted large original volume) suggests that it was produced by partial

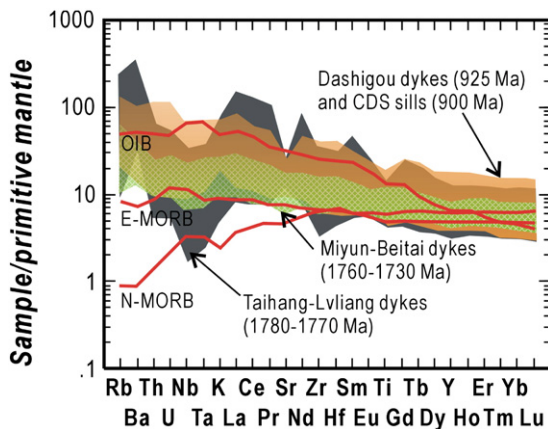


Fig. 7. Comparison of the Dashigou dykes and Chulan-Dalian-Sariwon (CDS) sills with the 1780–1770 Ma Taihang-Lvliang dykes (after Peng et al., 2007), 1760–1730 Ma Miyun-Beitai dykes (after Peng et al., 2011b) and ocean island basalts (OIB), enriched-mid ocean ridge basalts (E-MORB) and normal-MORB (N-MORB) (Sun and McDonough, 1989).

melting of a large mantle source area in the early Neoproterozoic. A link with a mantle plume is suggested by the E-MORB to OIB chemistry and associated radiating dyke swarm (e.g., Campbell, 2001; Ernst and Buchan, 2003).

There are several generations of Precambrian magmatism in the NCC after the formation of the SCLM, i.e., 1780–1730 Ma (Peng, 2010 and reference therein; Peng et al., 2011b), 1730–1680 Ma and ca. 1620 Ma (e.g. Li et al., 1995; Lu and Li, 1991; Lu et al., 2008; Ramö et al., 1995; Yu et al., 1996; Zhang et al., 2007; Zhao et al., 2004, 2009), 1350–1310 Ma (Li et al., 2009; Zhang et al., 2009c), and 925–900 Ma (this study). Among them, the 1780–1730 Ma Taihang (–Lvliang–Miyun–Beitai) dyke swarms and the 925–900 Ma Dashigou dyke swarm are of craton-scale; whereas the others are more locally distributed in the northern margin of the NCC (Fig. 1). Both of these (the 1780–1730 Ma and 925–900 Ma events) seem to have involved cratonic scale mantle upwelling through the SCLM, and this could have partly altered and weakened the SCLM, before its eastern part finally deconstructed (delaminated?) during the Mesozoic (e.g., Davis et al., 2001; Gao et al., 2004; Menzies et al., 1993, 2007; Rudnick et al., 2004; Wilde et al., 2003; Wu et al., 2008a; Yang et al., 2008; Zhang et al., 2002). In particular, the 925–900 Ma event centered in the southern margin of the eastern NCC could have specifically contributed to the mobilization and deconstruction of the SCLM, as this deconstruction mainly happened on the eastern side of the craton. Actually, the Nd isotope data of the late Paleozoic to early Mesozoic ultramafic rocks (data of Zhang et al., 2009a; Fig. 6) support derivation from the mobilized SCLM of the NCC, although it is possible that they were derived from subducted lithosphere of the Central Asian Ocean or asthenosphere (cf., Ernst et al., 2007; Miao et al., 2008; Xiao et al., 2003; Zhang et al., 2009a, b).

7.3. Relationship to the Bayan Obo REE ore deposit?

At the northern edge of the NCC, there is a world-class large REE ore deposit, Bayan Obo (or Bayun Obo, Baiyun'obo). Its time of emplacement and age of mineralization have long been debated, e.g., late Mesoproterozoic (~1200 Ma, e.g., Yuan et al., 1992; Ren et al., 1994; Zhang et al., 1994, 2001; Liu et al., 2005b; Le Bas, 2006; Yang et al., 2011), early Paleozoic (500–400 Ma, e.g., Ren et al., 1994; Wang et al., 1994; Chao et al., 1997; Qiao et al., 1997; Liu et al., 2004), and/or Neoproterozoic (ca. 800 Ma, e.g., Zhang et al., 2003). Although a majority believe that the age of main-stage mineralization could be late Mesoproterozoic, some think the mineralization possibly formed from a poly-phase process (e.g., Cao and Wang, 1994; Ren et al., 1994). That the ca. 920 Ma mafic dykes reach the northern margin of the NCC suggests a possible connection of the deposit to this specific magmatic event. The recently reported Early Neoproterozoic volcanics in the Langshan (Mts.) area of the Langshan-Bayan Obo Rift System (Peng et al., 2010) (Fig. 8a) may also be related. Perhaps the Bayan Obo intrusion and mineralization are part of the ~920 Ma events; this is allowed by available age constraints, but requires further evaluation.

7.4. Correlation of the 925–900 Ma dykes/sills in a global view

The widespread distribution and radiating geometry of the ca. 925 Ma dykes, with a focal point along the southern margin of the eastern NCC, as well as the ca. 900 Ma Xu-Huai Rift System that may represent part of a ‘triple junction’, suggest that additional ca. 925 Ma magmatism is likely present on the crustal block(s) that rifted away. The identification of matching ages of LIP magmatism on other blocks is a powerful tool for identifying former adjacent crustal blocks (Bleeker and Ernst, 2006).

Similar 920 Ma magmatism is reported from Congo and São Francisco cratons. In the West Congo craton, there are significant volcanics and sills

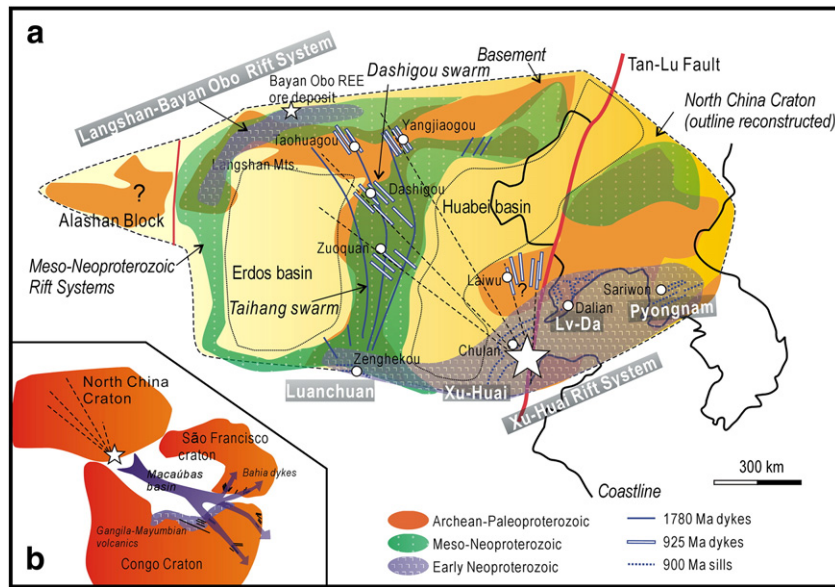


Fig. 8. a) A cartoon showing the reconstructed outline of the North China craton (after correction for Mesozoic strike-slip movement along the Tan-Lu fault) and the geometry of the 925 Ma mafic dykes and sills, as well as the Xu-Huai rift system; b) a provisional connection of the North China craton with the São Francisco-Congo craton at ca. 925 Ma. Distribution of the dykes in São Francisco-Congo craton and their flow directions (arrows) are after Correa-Gomes and Oliveira (2000). The distribution of the Gangila-Mayumbian volcanics is after Tack et al. (2001).

of ca. 920 Ma, e.g., the Gangila basalts, typical continental flood basalts, and subsequent Mayumbian rhyolitic lavas (dated at 920 ± 8 Ma at the base and 912 ± 7 Ma at the top; intruded by coeval high-level granites, e.g., the Mativa body at 924 ± 25 Ma and the Bata Kimenga body at 917 ± 14 Ma; ion microprobe U-Pb zircon ages) (Franssen and André, 1988; Tack et al., 2001). In the São Francisco craton (Brazil), dykes with ca. 920 Ma baddeleyite U-Pb ages have been reported (Bahia dykes, Evans et al., 2010; Correa-Gomes and Oliveira, 2000; Heaman, 1991), e.g., the Ondina dyke gives an age at 921.5 ± 4.3 Ma and the Meridian dyke at 924.2 ± 3.8 Ma (Evans et al., 2010). Correa-Gomes and Oliveira (2000) correlates the radiating Bahia dykes with those in Congo craton, suggesting a paleogeographic link. Marchak et al. (2006) suggested that the Macaúbas Basin at around 800 Ma was a Red Sea-type ocean formed between the São Francisco and Congo arms of the continent before this embayment area became a Pan-African orogen (the Araçuaí orogen) (see Macaúbas Basin in Fig. 8b).

Here we provisionally propose that these Bahia dykes in São Francisco craton and the Gangila-Mayumbian volcanics in the Congo craton could possibly be part of the same large igneous province as the Dashigou dyke swarm and CDS sills of the North China craton, on the basis of their precisely matched ages. Furthermore, the Macaúbas Basin may be the other arm of the triple conjunction (the Xu-Huai Rift System). Fig. 8b illustrates the provisional connection of these blocks, which awaits paleomagnetic testing.

8. Conclusions

The Dashigou dykes in the central part of the NCC give precise baddeleyite ages around 920 Ma, slightly older than some sills (ca. 900 Ma) along the southern margin but having comparable geochemistry. These dykes have a radiating geometry, with an apparent focal point centered along the southern margin of the NCC, where the early Neoproterozoic Xu-Huai Rift System likely constitutes two arms of a rift-rift-rift triple junction system. These dykes, as well as the sills, possibly originated from a mantle region other than the SCLM of the NCC, e.g., asthenosphere or deeper mantle, with significant assimilation/contamination from the lithosphere. Metasomatism might have occurred during the upwelling of the magma to produce these dykes and sills, and the SCLM of the NCC was possibly episodically (at least during 1780–1730 Ma and 925–

900 Ma events) mobilized prior to its eastern part mostly delaminating during the Mesozoic. A paleo-mantle plume origin is suggested for this ca. 925–900 Ma magmatism based on the radiating geometry of the dyke swarm, the associated Xu-Huai Rift System, and the OIB geochemistry of the rocks. Coeval associations comparable with the Dashigou dykes and CDS sills, and associated volcanics, exist on the São Francisco and Congo cratons. We therefore propose a provisional North China-São Francisco-Congo connection leading up to the ca. 925–900 Ma large igneous province magmatism and rifting.

Acknowledgments

This study was supported by NSFC project No. 41072146, 41030316 and 40730315. We are grateful to Drs. Mingguo Zhai, Jinghui Guo, Qiuli Li, Chaofeng Li and Fu Liu for their constructive advice and help. Two anonymous reviewers are thanked for their suggestions that greatly helped to improve this paper.

References

- Bleeker, W., Ernst, R., 2006. Short-lived mantle generated magmatic events and their dyke swarms: the key unlocking Earth's paleogeographic record back to 2.6 Ga. In: Hanski, E., Mertanen, S., Ramö, T., Vuollo, J. (Eds.), *Dyke Swarms – Time Markers of Crustal Evolution*. Taylor & Francis, London, pp. 3–26.
- Bryan, S., Ernst, R.E., 2008. Revised definition of large igneous provinces (LIPs). *Earth-Science Reviews* 86, 175–202.
- Bureau of Geology and Mineral Resources of Anhui (BGMRA), 1985. *Strata of Anhui (Precambrian part)*. Anhui Science and Technology Publishing House, Hefei, 174 pp.
- Campbell, I.H., 2001. Identification of ancient mantle plume. In: Ernst, R.E., Buchan, K.L. (Eds.), *Mantle Plumes: Their Identification through Time*. Geological Society of America, Special Papers, 352, pp. 5–21.
- Cao, R.-L., Wang, J.-W., 1994. Source materials for the Bayan Obo Fe-REE ore deposit and problems on the genetic theory. *Science in China. Series B* 24, 1298–1307.
- Chao, E.-C.-T., Back, J.M., Minkin, J.A., Tasumoto, M., Wang, J.-W., Conrad, J.E., Mckee, E.H., 1997. The sedimentary carbonate-hosted giant Bayan Obo REE-Fe-Nb ore deposit of Inner Mongolia, China: cornerstone examples for giant polymetallic ore deposits of hydrothermal origin. *USGS Bulletin* 2143, 65.
- Coffin, M.F., Eldholm, O., 1994. Large igneous provinces: crustal structure, dimensions and external consequences. *Reviews of Geophysics* 32, 1–36.
- Correa-Gomes, L.C., Oliveira, E.P., 2000. Radiating 1.0 Ga mafic dyke swarms of eastern Brazil and western Africa: evidence of post-assembly extension in the Rodinia supercontinent? *Gondwana Research* 3, 325–332.
- Cui, M.-L., Zhang, B.-L., Zhang, L.-C., 2011. U-Pb dating of baddeleyite and zircon from the Shizhaigou diorite in the southern margin of North China craton: constrains on

- the timing and tectonic setting of the Paleoproterozoic Xiong'er group. *Gondwana Research* 20, 184–193.
- Davis, D.W., 1982. Optimum linear regression and error estimation applied to U–Pb data. *Canadian Journal of Earth Sciences* 19, 2141–2149.
- Davis, G.A., Zheng, Y.D., Wang, C., Darby, B.J., Zhang, C.H., Gehrels, G.E., 2001. Mesozoic tectonic evolution of the Yanshan fold and thrust belt, with emphasis on Hebei and Liaoning Provinces, Northern China. In: Hendrix, M.S., Davis, G.A. (Eds.), *Paleozoic and Mesozoic Tectonic Evolution of Central Asia: From Continental Assembly to Intracontinental Deformation*: Geological Society of America Memoir, 194, pp. 171–197.
- Dewey, J.F., Burke, K.C.A., 1973. Hot spots and continental breakup: implications for collisional orogeny. *Geology* 2, 57–60.
- Ernst, R.E., Buchan, K.L., 2003. Recognizing mantle plumes in the geological record. *Annual Reviews of Earth and Planetary Sciences* 31, 469–523.
- Ernst, W.G., Tsujimori, T., Zhang, R., Liu, J.G., 2007. Permo-Triassic collision, Subduction-zone metamorphism, and tectonic exhumation along the East Asian continental margin. *Annual Review of Earth and Planetary Sciences* 35, 73–110.
- Evans, D.A.D., Heaman, L.M., Trindade, R.I.F., D'Agrella-Filho, M.S., Smirnov, A.V., Cotelani, E.L., 2010. Precise U–Pb baddeleyite ages from Neoproterozoic mafic dykes in Bahia, Brazil, and their paleomagnetic/paleogeographic implications, Abstract, GP31E-07. *American Geophysical Union, Joint Assembly, Meeting of the Americas, Iguassu Falls, August 2010*.
- Franssen, L., André, L., 1988. The Zadinian group (Late Proterozoic, Zaire) and its bearing on the origin of the West-Congo orogenic belt. *Precambrian Research* 38, 215–234.
- Gao, S., Rudnick, R.L., Carlson, R.-W., McDonough, W.-F., Liu, Y.-S., 2002. Re–Os evidence for replacement of ancient mantle lithosphere beneath the North China craton. *Earth and Planetary Science Letters* 198, 307–322.
- Gao, S., Rudnick, R.L., Yuan, H.-L., Liu, X.-M., Liu, Y.-S., Xu, W.-L., Ling, W.-L., Ayers, J., Wang, X.-C., Wang, Q.-H., 2004. Recycling lower continental crust in the North China craton. *Nature* 432, 892–897.
- Guo, J.-H., Sun, M., Chen, F.-K., Zhai, M.-G., 2005. Sm–Nd and SHRIMP U–Pb zircon geochronology of high-pressure granulites in the Sanggan area, North China craton: timing of Paleoproterozoic continental collision. *Journal of Asian Earth Sciences* 24, 629–642.
- Halls, H.C., Li, J.-H., Davis, D., Hou, G.-T., Zhang, B.-X., Qian, X.-L., 2000. A precisely dated Proterozoic paleomagnetic pole from the North China craton, and its relevance to paleocontinental construction. *Geophysical Journal International* 143, 185–203.
- Hanski, E., Mertanen, S., Rämö, T., Vuollo, J. (Eds.), 2006. *Dyke Swarms – Time Markers of Crustal Evolution*. Taylor & Francis Publisher, 273 pp.
- He, Y.-H., Zhao, G.-C., Sun, M., Xia, X.-P., 2009. SHRIMP and LA–ICP–MS zircon geochronology of the Xiong'er volcanic rocks: implications for the Paleo-Mesoproterozoic evolution of the southern margin of the North China craton. *Precambrian Research* 168, 213–222.
- Heaman, L., 1991. U–Pb dating of giant radiating dyke swarms: potential for global correlation of mafic magmatic events. *International Symposium on Mafic Dykes*. São Paulo, Brazil, Extended Abstracts, 3o Congresso Brasileira de Geoquímica - 10o Congresso de Geoquímica dos Países de Língua Portuguesa, pp. 7–9.
- Heaman, L.M., LeCheminant, A.N., 1993. Paragenesis and U–Pb systematics of baddeleyite (ZrO₂). *Chemical Geology* 110, 95–126.
- Heaman, L.M., LeCheminant, A.N., 2001. Anomalous U–Pb systematics in mantle-derived baddeleyite xenocrysts from Île Bizard: evidence for high temperature radon diffusion? *Chemical Geology* 172, 77–93.
- Hou, G.-T., Liu, Y.-L., Li, J.-H., Jin, A.-W., 2005. The SHRIMP U–Pb chronology of mafic dyke swarms: a case study of Laiwu diabase dykes in western Shandong. *Acta Petrologica et Mineralogica* 24 (3), 179–185 (in Chinese with English abstract).
- Hou, G.-T., Li, J.-H., Yang, M.-H., Yao, W.-H., Wand, C.-C., Wand, Y.-X., 2008. Geochemical constraints on the tectonic environment of the late Paleoproterozoic mafic dyke swarms in the North China craton. *Gondwana Research* 13, 103–116.
- Hu, J.-L., Zhao, T.-P., Xu, Y.-H., Chen, W., 2007. Geochemistry and petrogenesis of the high-K volcanic rocks in the Dahongyu formation, North China craton. *Journal of Mineralogy and Petrology* 12, 70–77 (in Chinese with English abstract).
- Irvine, T.N., Baragar, W.R.A., 1971. A guide to the chemical classification of the common volcanic rocks. *Canadian Journal of Earth Sciences* 8, 523–548.
- Kröner, A., Wilde, S.A., Li, J.-H., Wang, K.-Y., 2005. Age and evolution of a Late Archaean to Paleoproterozoic upper to lower crustal section in the Wutaishan/Hengshan/Fuping terrain of North China. *Journal of Asian Earth Sciences* 24, 576–595.
- Kröner, A., Wilde, S.A., Zhao, G.-C., O'Brien, P.J., Sun, M., Liu, D.-Y., Wan, Y.-S., Liu, S.-W., Guo, J.-H., 2006. Zircon geochronology and metamorphic evolution of mafic dykes in the Hengshan Complex of northern China: evidence for late Paleoproterozoic extension and subsequent high-pressure metamorphism in the North China craton. *Precambrian Research* 146, 45–67.
- Kumarapeli, P.S., 1993. A plume-generated segment of the rifted margin of Laurentia, Southern Canadian Appalachians, seen through a completed Wilson Cycle. *Tectonophysics* 219, 47–55.
- Kusky, T.M., Li, J.-H., 2003. Paleoproterozoic tectonic evolution of the North China craton. *Journal of Asian Earth Sciences* 22, 383–397.
- Kusky, T.M., Li, J.-H., Tucker, R.T., 2001. The Archaean Dongwanzi ophiolite complex, North China craton: 2.505 billion year old oceanic crust and mantle. *Science* 292, 1142–1145.
- Kusky, T., Li, J.-H., Santosh, M., 2007. The Paleoproterozoic North Hebei Orogen: North China craton's collisional suture with the Columbia supercontinent. *Gondwana Research* 12, 4–28.
- Le Bas, M.J., 2006. Re-interpretation of zircon date in a carbonatite dyke at the Bayan Obo giant REE–Fe–Nb deposit, China. *Acta Petrologica Sinica* 22, 517–518 (in Chinese with English abstract).
- Li, H.-K., Li, H.-M., Lu, S.-N., 1995. Grain zircon U–Pb ages for volcanic rocks from Tuanshanzi Formation of Changcheng System and their geological implications. *Geochemica* 24, 43–48 (in Chinese with English abstract).
- Li, J.-H., Qian, X.-L., Huang, X.-N., Liu, S.-W., 2000. Tectonic framework of North China block and its cratonization in the Early Precambrian. *Acta Petrologica Sinica* 16, 1–10 (in Chinese with English abstract).
- Li, J.-H., Kusky, T.M., Huang, X.-N., 2002. Neoproterozoic podiform chromitites and mantle tectonites in ophiolitic mélange, North China craton: a record of early oceanic mantle processes. *GSA Today* 12, 4–11.
- Li, H.-K., Lu, S.-N., Li, H.-M., Sun, L.-X., Xiang, Z.-Q., Geng, J.-Z., Zhou, H.-Y., 2009. Zircon and baddeleyite U–Pb precision dating of basic rock sills intruding Xiamaling Formation, North China. *Geological Bulletin of China* 28 (10), 1396–1404 (in Chinese with English Abstract).
- Li, Q.L., Li, X.H., Liu, Y., Tang, G.Q., Yang, J.H., Zhu, W.G., 2010. Precise U–Pb and Pb–Pb dating of Phanerozoic baddeleyite by SIMS with oxygen flooding technique. *Journal of Analytical Atomic Spectrometry* 25, 1107–1113.
- Liu, D.-Y., Nutman, A.P., Compston, W., Wu, J.-S., Shen, Q.-H., 1992. Remnants of 3800 Ma crust in the Chinese part of the Sino–Korean craton. *Geology* 20, 339–342.
- Liu, Y.-L., Yang, G., Chen, J.-F., Du, A.-D., Xie, Z., 2004. Re–Os dating of pyrite from Giant Bayan Obo REE–Nb–Fe deposit. *Chinese Science Bulletin* 49, 2627–2631.
- Liu, S.-W., Pan, Y.-M., Xie, Q.-L., Zhang, J., Li, Q.-G., Yang, B., 2005a. Geochemistry of the Paleoproterozoic Nanyang granitic gneisses in the Fuping Complex: implications for the tectonic evolution of the Central Zone, North China craton. *Journal of Asian Earth Sciences* 24, 643–658.
- Liu, Y.-L., Chen, J.-F., Li, H.-M., Qian, H., Xiao, G.-W., Zhang, T.-R., 2005b. Single-grain U–Th–Pb–Sm–Nd dating of monazite from dolomite type ore of the Bayan Obo deposit. *Acta Petrologica Sinica* 21, 881–888 (in Chinese with English abstract).
- Liu, S.-W., Zhao, G.-C., Wilde, S.A., Shu, G.-M., Sun, M., Li, Q.-G., Tian, W., Zhang, J., 2006a. Th–U–Pb monazite geochronology of the Lvliang and Wutai Complexes: constraints on the tectonothermal evolution of the Trans-North China Orogen. *Precambrian Research* 148, 205–225.
- Liu, Y.-Q., Gao, L.-Z., Liu, Y.-X., Song, B., Wang, Z.-X., 2006b. Zircon U–Pb dating for the earliest Neoproterozoic mafic magmatism in the southern margin of the North China Block. *Chinese Science Bulletin* 51, 2375–2382.
- Liu, D.-Y., Wilde, S., Wan, Y.-S., Wu, J.-S., Zhou, H.-Y., Dong, C.-Y., Yin, X.-Y., 2008. New U–Pb and Hf isotopic data confirm Anshan as the oldest preserved segment of the North China craton. *American Journal of Science* 308, 200–231.
- Lu, S.N., Li, H.M., 1991. Zircon age of Dahongyu Formation. *Bulletin of Chinese Academy of Geological Sciences* 22, 137–145 (in Chinese with English abstract).
- Lu, S.N., Zhao, G.C., Wang, H.C., et al., 2008. Precambrian metamorphic basement and sedimentary cover of the North China craton: a review. *Precambrian Research* 160, 77–93.
- Ludwig, K.R., 2003. *User's manual for Isoplot/EX version 3.00*. A Geochronological Toolkit for Microsoft Excel, vol. 4. Berkeley Geochronology Centre Special Publication, 71 pp.
- Marchak, S., Alkmim, F.F., Whittington, A., Pedrosa-Soares, A.C., 2006. Extensional collapse in the Neoproterozoic Araçuaí orogen, eastern Brazil: a setting for reactivation of asymmetric cratonization cleavage. *Journal of Structural Geology* 28, 129–147.
- Matthews, W., Davis, W.J., 1999. A practical image analysis technique for estimating the weight of abraded mineral fractions used in U–Pb dating. *Radiogenic Age and Isotopic Studies: Geological Survey of Canada, Current Research 1999-F: Report*, 12, pp. 1–7.
- Menzies, M.A., Fan, W.M., Zhang, M., 1993. Palaeozoic and Cenozoic lithosphere and the loss of N 120 km of Archaean lithosphere, Sino–Korean craton, China. In: Prichard, H.M., Alabaster, T., Harris, N.B.W., Neary, C.R. (Eds.), *Magmatic Processes and Plate Tectonics: Geological Society Special Publication*, 76, pp. 71–81.
- Menzies, M., Xu, Y.G., Zhang, H.F., Fan, W.M., 2007. Integration of geology, geophysics and geochemistry: a key to understanding the North China craton. *Lithos* 96, 1–21.
- Miao, L.C., Fan, W.M., Liu, D.Y., Zhang, F.Q., Shi, Y.R., Guo, F., 2008. Geochronology and geochemistry of the Hegenshan ophiolitic complex: implications for late-stage tectonic evolution of the Inner Mongolia–Daxinganling Orogenic Belt, China. *Journal of Asian Earth Sciences* 32, 348–370.
- Parrish, R.R., 1987. An improved micro-capsule for zircon dissolution in U–Pb geochronology. *Chemical Geology* 66, 99–102.
- Peng, P., 2005. *Petrogenesis and Tectonic Significance of the ca. 1.8 Ga Mafic Dyke Swarms in the Central North China craton*. PhD thesis of the Institute of Geology and Geophysics, Chinese Academy of Sciences, Beijing, 213 pp.
- Peng, P., 2010. Reconstruction and interpretation of giant mafic dyke swarms: a case study of 1.78 Ga magmatism in the North China craton. In: Kusky, T., Zhai, M.-G., Xiao, W.-J. (Eds.), *The Evolving Continents: Understanding Processes of Continental Growth*: Geological Society, London, Special Publication, 338, 163–178.
- Peng, P., Zhai, M.-G., Zhang, H.-F., Zhao, T.-P., Ni, Z.-Y., 2004. Geochemistry and geological significance of the 1.8 Ga mafic dyke swarms in the North China craton: an example from the juncture of Shanxi, Hebei and Inner-Mongolia. *Acta Petrologica Sinica* 20, 439–456.
- Peng, P., Zhai, M.-G., Guo, J.-H., Kusky, T., Zhao, T.-P., 2007. Nature of mantle source contributions and crystal differentiation in the petrogenesis of the 1.78 Ga mafic dykes in the central North China craton. *Gondwana Research* 12, 29–46.
- Peng, P., Zhai, M., Ernst, R., Guo, J., Liu, F., Hu, B., 2008. A 1.78 Ga large igneous province in the North China craton: the Xiong'er Volcanic Province and the North China dyke swarm. *Lithos* 101 (3–4), 260–280.
- Peng, R.-M., Zhai, Y.-S., Wang, J.-P., Chen, X.-F., Liu, Q., Lv, J.-F., Shi, Y.-X., Wang, G., Li, S.-W., Wang, L.-G., Ma, Y.-T., Zhang, P., 2010. Discovery of Neoproterozoic acid volcanic rock in the south-western section of Langshan, Inner Mongolia. *Chinese Science Bulletin* 55, 2611–2620 (in Chinese).
- Peng, P., Zhai, M., Li, Q., Wu, F., Hou, Q., Li, Z., Li, T., Zhang, Y., 2011a. Neoproterozoic (900 Ma) Sariwon sills in North Korea: geochronology, geochemistry and implications for the evolution of the south-eastern margin of the North China craton. *Gondwana Research* 20, 243–254.

- Peng, P., Liu, F., Zhai, M.-G., Guo, J.-H., 2011b. Age of the Miyun dyke swarm: constraints on the maximum depositional age of the Changcheng System. *Chinese Science Bulletin* 56. doi:10.1007/s11434-011-4771-x.
- Qiao, X., Gao, L.-Z., Peng, Y., Zhang, Y.-B., 1997. The stratigraphy of Sailinghudong group and ore-bearing micrite mound in Bayan Obo, Inner Mongolia. *Acta Geologica Sinica* 71, 202–211.
- Ramö, O.T., Haapala, I., Vaasjoki, M., Yu, J.H., Fu, H.Q., 1995. The 1700 Ma Shachang complex, northeast China: Proterozoic rapakivi granite not associated with Paleoproterozoic orogenic crust. *Geology* 23, 815–818.
- Ren, Y., Zhang, Y., Zhang, Z., 1994. Study on heat events of ore forming in the Bayan Obo deposit. *Scientia Geologica Sinica* 29, 95–101 (in Chinese with English abstract).
- Roddick, J.C., Loveridge, W.D., Parrish, R.R., 1987. Precise U–Pb dating of zircon at the sub-nanogram Pb level. *Chemical Geology* 66, 111–121.
- Rudnick, R.L., Gao, S., Ling, W.L., Liu, Y.S., McDonough, W., 2004. Petrology and geochemistry of spinel peridotite xenoliths from Hannuoba and Qixia, North China craton. *Lithos* 77, 609–637.
- Söderlund, U., Johansson, L., 2002. A simple way to extract baddeleyite (ZrO₂). *Geochemistry Geophysics Geosystems* 3 number 2.
- Stacey, J.S., Kramers, J.D., 1975. Approximation of terrestrial lead isotope evolution by a two-stage model. *Earth and Planetary Science Letters* 26, 207–221.
- Sun, S.-S., McDonough, W.F., 1989. Chemical and isotopic systematics of oceanic basalts implications for mantle composition and process. In: Saunders, A.D., Nony, M.J. (Eds.), *Magmatism in the Ocean Basins: Geological Society Special Publication*, 42, pp. 313–354.
- Tack, L., Wingate, M.T.D., Liégeois, J.-P., Fernandez-Alonso, M., 2001. Early Neoproterozoic magmatism (1000–910 Ma) of the Zadinian and Mayumbian Groups (Bas-Congo): onset of Rodinia rifting at the western edge of the Congo craton. *Precambrian Research* 110, 277–306.
- Wang, J.-W., Tatsumoto, M., Li, X.-B., Premo, W.R., Chao, E.-C.-T., 1994. A precise Th-232–Pb-208 chronology of fine-grained monazite-age of the Bayan Obo REE–Fe–Nb ore deposit, China. *Geochimica et Cosmochimica Acta* 58, 3155–3169.
- Wang, Y.-J., Fan, W.-M., Zhang, Y.-H., Guo, F., Zhang, H.-F., Peng, T.-P., 2004. Geochemical, ⁴⁰Ar/³⁹Ar geochronological and Sr–Nd isotopic constraints on the origin of Paleoproterozoic mafic dikes from the southern Taihang Mountains and implications for the ca. 1800 Ma event of the North China craton. *Precambrian Research* 135, 55–77.
- Wang, Y.-J., Zhao, G.-C., Cawood, P.A., Fan, W.-M., Peng, T.-P., Ssun, L.-H., 2008. Geochemistry of Paleoproterozoic (1770 Ma) mafic dikes from the Trans-North China Orogen and tectonic implications. *Journal of Asian Earth Sciences* 33, 61–77.
- Wilde, S.A., Zhao, G.-C., Sun, M., 2002. Development of the North China craton during the Late Archean and its final amalgamation at 1.8 Ga: some speculation on its position within a global Paleoproterozoic Supercontinent. *Gondwana Research* 5, 85–94.
- Wilde, S.A., Zhou, X.H., Nemchin, A.A., Sun, M., 2003. Mesozoic crust–mantle interaction beneath the North China craton: a consequence of the dispersal of Gondwanaland and accretion of Asia. *Geology* 31, 817–820.
- Wu, F.-Y., Zhao, G.-C., Wilde, S.A., Sun, D.-Y., 2005. Nd isotopic constraints on crustal formation in the North China craton. *Journal of Asia Earth Sciences* 24 (5), 523–546.
- Wu, F.-Y., Xu, Y.-G., Gao, S., Zheng, J.-P., 2008a. Lithospheric thinning and destruction of the North China craton. *Acta Petrologica Sinica* 24, 1145–1174 (in Chinese with English abstract).
- Wu, F.-Y., Zhang, Y.-B., Yang, J.-H., Xie, L.-W., Yang, Y.-H., 2008b. Zircon U–Pb and Hf isotopic constraints on the Early Archean crustal evolution in Anshan of the North China craton. *Precambrian Research* 167 (3–4), 339–362.
- Xiao, W., Windley, B.F., Hao, J., Zhai, M.G., 2003. Accretion leading to collision and the Permian Solonker suture, Inner Mongolia, China: termination of the central Asian orogenic belt. *Tectonics* 22, 1069. doi:10.1029/2002TC001484.
- Xie, G.H., 2005. *Petrology and Geochemistry of the Damiao Anorthosite and the Miyun Rapakivi Granite*. Scientific Press, Beijing, 195 pp. (in Chinese).
- Xu, J.-W., Zhu, G., 1995. Discussion on tectonic models for the Tan–Lu fault zone, Eastern China. *Journal of Geology and Mineral Resources of North China* 10, 121–133 (in Chinese).
- Xu, J.W., Zhu, G., Tong, W., Cui, K., Liu, Q., 1987. Formation and evolution of the Tancheng–Lujiang wrench fault system: a major shear system to the northeast of the Pacific Ocean. *Tectonophysics* 134, 273–310.
- Yan, G.-H., Cai, J.-H., Ren, K.-X., Liu, C.-X., Liu, X.-Y., Mu, B.-L., Yang, B., Li, F.-T., Huang, B.-L., Ma, F., 2010. SHRIMP U–Pb zircon ages of the trachyte in the Dahongkou Formation, Luanchuan Group, southern margin of the North China craton. *National Petrology and Geodynamic Conference Abstract Volume (Beijing) 2010*, 289–290.
- Yang, J.H., Wu, F.Y., Liu, X.M., Xie, L.W., 2005. Zircon U–Pb ages and Hf isotopes and their geological significance of the Miyun rapakivi granites from Beijing, China. *Acta Petrol. Sinica* 21 (6), 1633–1644 (in Chinese with English abstract).
- Yang, J.-H., Wu, F.-Y., Wilde, S.A., Belousova, E., Griffin, W.L., 2008. Mesozoic decratonization of the North China Block. *Geology* 36, 467–470.
- Yang, K.-F., Fan, H.-R., Santosh, M., Hu, F.-F., Wang, K.-Y., 2011. Mesoproterozoic mafic and carbonatitic dykes from the northern margin of the North China craton: implications for the final breakup of Columbia supercontinent. *Tectonophysics* 498, 1–10.
- Ye, K., Cong, B., Ye, D.-N., 2000. The possible subduction of continental material to depths greater than 200 km. *Nature* 407, 734–736.
- Ye, K., Song, Y.-R., Chen, Y., Xu, H.-J., Liu, J.-B., Sun, M., 2009. Multistage metamorphism of orogenic garnet–lherzolite from Zhimafang, Sulu UHP terrane, E. China: implications for mantle wedge convection during progressive oceanic and continental subduction. *Lithos* 109, 155–175.
- Yu, J.H., Fu, H.Q., Zhang, F.L., Wan, F.X., Haapala, I., Ramo, O.T., Vaasjoki, M., 1996. Anorogenic Rapakivi Granite and Related Rocks in the Northern Part of North China craton. *China Sci. Technol. Press, Beijing*, 189 pp. (in Chinese with English abstract).
- Yuan, Z.-X., Bai, G., Wu, C.-Y., Zhang, Z.-Q., Ye, X.-J., 1992. Geological features and genesis of the Bayan Obo REE ore deposit, Inner-Mongolia, China. *Applied Geochemistry* 7, 429–442.
- Zhai, M.G., Liu, W.J., 2003. Paleoproterozoic tectonic history of the North China craton: a review. *Precambrian Research* 122, 183–199.
- Zhai, M.-G., Santosh, M., 2011. The early Precambrian odyssey of North China craton: a synoptic overview. *Gondwana Research* 20, 6–25.
- Zhai, M.G., Guo, J.-H., Liu, W.-J., 2005. Neoproterozoic continental evolution and tectonic history of the North China craton: a review. *Journal of Asian Earth Sciences* 24, 547–562.
- Zhai, M.-G., Guo, J.-H., Li, Z., Chen, D.-Z., Peng, P., Li, T.-S., Hou, Q.-L., Fan, Q.-C., 2007. Linking the Sulu UHP belt to the Korean Peninsula: evidence of eclogite, Precambrian basement, and Paleozoic sedimentary basins. *Gondwana Research* 12, 388–403.
- Zhang, Z.-Q., Tang, S., Wang, J., Yuan, Z.-X., Bai, G., 1994. New data of the formation ages for the Bayan Obo REE deposit. *Acta Geoscientia Sinica* 29, 85–94 (in Chinese with English abstract).
- Zhang, Z.-Q., Tang, S.-H., Yuan, Z.-X., Bai, G., Wang, J.-H., 2001. The Sm–Nd and Rb–Sr isotopic systems of the dolomites in the Bayan Obo deposit, Inner Mongolia, China. *Acta Petrologica Sinica* 17, 637–642 (in Chinese with English abstract).
- Zhang, H.-F., Sun, M., Zhou, X.-H., Fan, W.-M., Zhai, M.-G., Yin, J.-F., 2002. Mesozoic lithosphere destruction beneath the North China craton: evidence from major, trace element, and Sr–Nd–Pb isotope studies of Fangcheng basalts. *Contributions to Mineralogy and Petrology* 144, 241–253.
- Zhang, Z.-Q., Tang, S.-H., Wang, J.-H., Yuan, Z.-X., Bai, G., 2003. Information about ore deposit formation in different epochs: age of the west orebodies of the Bayan Obo deposit with a discussion. *Geology in China* 30, 130–137 (in Chinese with English abstract).
- Zhang, S.-H., Liu, S.-W., Zhao, Y., Yang, J.-H., Song, B., Liu, X.-M., 2007. The 1.75–1.68 Ga anorthosite–mangerite–alkali granitoid–rapakivi granite suite from the northern North China craton: magmatism related to a Paleoproterozoic orogen. *Precambrian Research* 155, 287–312.
- Zhang, S.-H., Zhao, Y., Liu, X.-C., Liu, D.-Y., Chen, F.-K., Xie, L.-W., Chen, H.-H., 2009a. Late Paleozoic to Early Mesozoic mafic–ultramafic complexes from the northern North China Block: constraints on the composition and evolution of the lithospheric mantle. *Lithos* 110, 229–246.
- Zhang, S.-H., Zhao, Y., Song, B., Hu, J.-M., Liu, S.-W., Yang, Y.-H., Chen, F.-K., Liu, X.-M., Liu, J., 2009b. Contrasting Late Carboniferous and Late Permian–Middle Triassic intrusive suites from the northern margin of the North China craton: geochronology, petrogenesis and tectonic implications. *Geological Society of America Bulletin* 121, 181–200.
- Zhang, S.-H., Zhao, Y., Yang, Z.-Y., He, Z.-F., Wu, H., 2009c. The 1.35 Ga diabase sills from the northern North China craton: implications for breakup of the Columbia (Nuna) supercontinent. *Earth and Planetary Science Letters* 288, 588–600.
- Zhao, G.-C., Wilde, S.A., Cawood, P.A., Lu, L.-Z., 1998. Thermal evolution of the Archean basement rocks from the eastern part of the North China craton and its bearing on tectonic setting. *International Geology Review* 40, 706–721.
- Zhao, G.-C., Wilde, S.A., Cawood, P.A., Sun, M., 2001. Archean blocks and their boundaries in the North China craton: lithological, geochemical, structural and P–T path constraints and tectonic evolution. *Precambrian Research* 107, 45–73.
- Zhao, T.-P., Zhou, M.-F., Zhai, M.-G., Xia, B., 2002. Paleoproterozoic rift-related volcanism of the Xiong'er group, North China craton: implications for the breakup of Columbia. *International Geology Review* 44, 336–351.
- Zhao, T.P., Chen, F.K., Zhai, M.G., Xia, B., 2004. Single zircon U–Pb ages and their geological significance of the Damiao anorthosite complex, Heibei Province, China. *Acta Petrologica Sinica* 20, 685–690 (in Chinese with English abstract).
- Zhao, G.-C., Sun, M., Wilde, S.A., Li, S.-Z., 2005. Late Archean to Paleoproterozoic evolution of the North China craton: key issues revisited. *Precambrian Research* 136, 177–202.
- Zhao, T.-P., Chen, W., Zhou, M.-F., 2009. Geochemical and Nd–Hf isotopic constraints on the origin of the 1.74 Ga Damiao anorthosite complex, North China craton. *Lithos* 113, 673–690.